American Journal of Construction and Building Materials
2022; 6(1): 17-42
http://www.sciencepublishinggroup.com/j/ajcbm
doi: 10.11648/j.ajcbm.20220601.13
ISSN: 2640-0022 (Print); ISSN: 2640-0057 (Online)

Determination of Water Level on the Reservoir of the Earthen Dam of Songloulou Based on the Artificial Neural Network and Assessment of the Stress and Displacements

Amba Jean Chills[1, 2], Zoa Ambassa[1, 2, *], Offolé Florence[1], Essola Dieudonné[1], Bodol Momha Merlin[1], Nzengwa Robert[1], Mbongo Pascal Adrien[3]

[1]Laboratory of Energy Modeling Materials and Methods (E3M), National Higher Polytechnic School of Douala, University of Douala, Douala, Cameroon

[2]Department of Civil Engineering, National Higher Polytechnic School of Douala, University of Douala, Douala, Cameroon

[3]The Energy of Cameroon (ENEO), Douala, Cameroon

Email address:

jc.amba@enspd-udo.cm (A. J. Chills), daniel.zoa77@yahoo.fr (Z. Ambassa)

[*]Corresponding author

To cite this article:

Amba Jean Chills, Zoa Ambassa, Offolé Florence, Essola Dieudonné, Bodol Momha Merlin, Nzengwa Robert, Mbongo Pascal Adrien. Determination of Water Level on the Reservoir of the Earthen Dam of Songloulou Based on the Artificial Neural Network and Assessment of the Stress and Displacements. *American Journal of Construction and Building Materials*. Vol. 6, No. 1, 2022, pp. 17-42.
doi: 10.11648/j.ajcbm.20220601.13

Received: April 27, 2022; **Accepted**: May 14, 2022; **Published**: May 26, 2022

Abstract: In this paper, we used artificial intelligence for the analysis of water level and displacements data from the Songloulou earth dam of Cameroon. Measurements of safety and reliability indicators follow changes dictated by several reversible and irreversible phenomena like piezometric and pendulums measurements. The results obtained over many years have confirmed the relevance and robustness of models using artificial intelligence. We have simulated the behavior model through piezometric and pendulum measurements of this dam more precisely the ANFIS (Adaptive Neural Fuzzy Inference System) model, which combines the concept of artificial neurons and that of fuzzy logic, has provided satisfactory results, given the large amount of data to be processed. The water level evolution is modeled using the ANFIS function integrated in the MATLAB software and we compare it with the HST (Hydrostatic Season Time) method. Afterwards, the stress state of the structure is evaluated based on the hydromechanical behavior using the PLAXIS Finite Element calculation code. In this case, the input parameters are: the hydraulic heads recorded on the piezometers and geotechnical parameters of the dam. The modeling results in terms of displacement are perfectly consistent with the displacement measurements. The horizontal displacement obtained in the model at the pendulums position is 80 mm and that of the pendulums is 70 mm of average value.

Keywords: Earth Dam, Artificial Intelligence, Piezometers, Pendulums, ANFIS, HST, MATLAB, PLAXIS

1. Introduction

The evaluation and analysis of the monitoring data of a dam during its lifetime make it possible to process the influence of external parameters on these measurements [1-4]. Indeed, the variations in measurements recorded on the dam's result from a combination of immediately inseparable factors, whatever the nature and the sophistication of the monitoring instruments used [5-9]. Three factors are preponderant; two of them are reversible if the stability or resistance limits are not reached: the hydrostatic conditions, i.e. the water level in the reservoir and the climatic conditions (temperature, rain, water content) [5-9]. The third irreversible is related to the age of the dam [5-9]. A real analysis of the structure assumes that we can follow the evolution of its behavior over time, after deducting any other variation [1-9]. The first step consists in displaying the measurements of each instrument on a graph adapted to the phenomenon to be analyzed: in general several years for the mechanical quantities, and according to the retention level for the hydraulic quantities, by also showing the threshold to check

that there is no read error [5-14]. This first level of analysis most often makes it possible to detect, at least qualitatively, sudden and even slow irreversible variations, in particular when there are few explanatory factors (restraint at an almost constant level, measurements not subject to seasonal influences). However, this level of analysis turns out to be insufficient, in particular for the largest dams, as soon as one wishes to access numerical values within reasonable time or when several explanatory factors coexist; more sophisticated statistical models are used. Moreover, this level of analysis may prove to be insufficient when one wishes to access numerical values. For this category of structures, the importance of rapid processing of auscultation data considered essential for the analysis of overall or partial stability of the dam is obvious [15-17]. It is advisable to use deterministic models or even statistical models to improve the reliability of the measurements.

Regarding deterministic models, finite element calculation models are commonly used at the dam project stage [15]. Indeed, subject to a good knowledge of the parameters of material behavior laws, they make it possible to reliably represent the deformations and stresses in the embankment in different project situations. They also make it possible to assess the state of stress during the life of the structure, especially in the context of safety reassessment studies [18-25]. The limits of these approach lies in the fact that the calculations are quite laborious when one wishes to model the regular monitoring of the structure and, above all, they do not easily allow the consideration of the complexity of the factors which influence the nonlinear behavior and the heterogeneities of soil, rock and concrete materials.

However, the statistical analysis methods for auscultation measurements seem more advantageous because they make it possible to separate the respective influences of several explanatory factors introduced into the model. Among them, we can cite the 'HST' method which was originally developed for the pendulums of arch dams (Carrere). From this method arise approaches such as the 'ACP' method which has the advantage of establishing the links between several variables, by quantifying their correlations with the main components of the sample. These methods and their derivatives are used in several countries and their field of application has considerably expanded.

On the other hand, for the particular case of hydraulic measurements (piezometry and flow rates), a hysteresis effect is commonly observed when representing the value of the pore pressure in the core or an earth dam foundation, as a function of the coast of restraint. Indeed, the path described when going up the body of water is not the same as the way down. Bonelli and collective [1, 6-8] explain this phenomenon by the fact that the soil capacity is never null, because the presence of dissolved or occluded air, even for compacted soils close to saturation. Thus, compared to the models described above, taking into account the delayed response seems more suitable for analyzing data when there is a difference between the solicitation and the response measured by the monitoring instrument.

Despite this consideration of the delayed response, it can be seen that the modeling of the evolution of the measured parameters does not agree perfectly with the real data. This delayed effect is more suitable for embankment dams but for concrete dams the modeling seems more delicate given the number of parameters to be considered [6, 7].

In order to minimize the error made in the analysis of a set of data, the neural network approach is a solution to overcome the limitations of the methods mentioned above. It is a recent method proposed to also respond to the two limitations of the HST method, namely the strong assumption of decoupling of actions, linked to that of the linearity of the HST model and the highlighting of delayed actions. Indeed, the neural network method makes it possible to model nonlinearities based on the use of the properties of time series [26]. These non-linearities are closely linked to the evolution of geotechnical parameters, environmental parameters, as well as structural parameters of the dam.

2. Presentation of Structures and Context of Research

2.1. Presentation of the Songloulou Hydroelectric Earthen Dam

The Songloulou large earthen dam (Figure 1) is located in the Littoral region of Cameroon, towards Babimbi, near Massok. It was implanted on the Sanaga River. With its vast watershed representing more than 25% of the total area of the country and its many rapids, the Sanaga is the largest river in Cameroon and constitutes a reservoir of hydroelectric energy of the first order. The main dam, leveled at height 530 m, and has a central sealing core in compacted lateritic clay, separated from the upstream and downstream rock fill by sand and gravel filters. A riprap zone with large rockfill provides anti-swing protection on the upstream face and a 9 m wide crest.

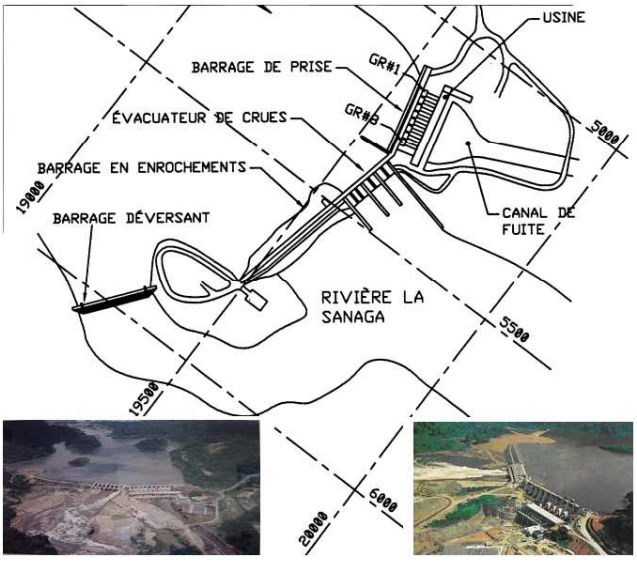

Figure 1. *General view of the Songloulou hydroelectric development.*

The spillway is calculated to evacuate an exceptional flood of 10,000 m^3/s below elevation 528.50 m with a blocked valve. It has seven passes closed by segment gates 14 m wide and 17 m high, controlled by winches and chains. The passes, whose sill is at elevation 511 m, are separated by pillars 4.5 m thick, which support the valve equipment rooms at elevation 530 m. The intake dam, with a maximum height of 35 m, is made up of eight sluices 13.5 m wide separated by buttresses, a connecting gravity wall to the left bank and a connecting buttress structure at the spillway. The openings of the four intakes on the left bank are equipped with large screens, cleaned by a bar screen rolling on the crown of the structure at elevation 530.

2.2. Context and Issue

Concrete swelling phenomena were identified six years after the commissioning of the first units (1981) by reducing the clearances between the fixed and moving parts of the turbines and alternators. These swellings had various consequences, making the operation and safety of the structures difficult. Studies have been undertaken since 1991, aimed at evaluating and improving the safety of the structures, as well as a series of interventions to counter the effects of swelling on the equipment with increased auscultation for the monitoring of the structures [27]. On the Songloulou development, monitoring data is regularly collected but the site has no means of analyzing this data automatically. Analyzing these auscultation data raises questions about the effective technique to use given the advantages and limitations of monitoring techniques. The objective of this article is to analyze the auscultation data of the Songloulou hydroelectric dam using artificial intelligence and to propose a method of prediction and assistance in the analysis of said data for the operation of the structure safe.

3. Monitoring Data Analysis Methodology

The Songloulou hydroelectric dam has within it 12 pendulums to measure displacements, 40 piezometers for pressures and more than 200 other monitoring devices. In this paper we are interested in the analysis of sub-pressures and horizontal displaments on concrete structures, that is to say the intake dam and the spillway dam. The layout of the piezometric devices in these two works is illustrated in Figures 2 to 5. The methodology consists of analyzing this quantity of data collected on the site at regular intervals for more than a decade using artificial intelligence models. Several research works have been carried out around the world using these techniques to guarantee the reliability and safety of dams [26-34].

On the intake dam, 30 piezometers are usable out of the 31 installed. On the gallery spillway dam, 09 piezometers can be used. These structures are subject to regular monitoring. We are interested in the behavior of this dam during the period from 1997 to 2019 for the pendulum data and from 2008 to 2019 for the piezometric data.

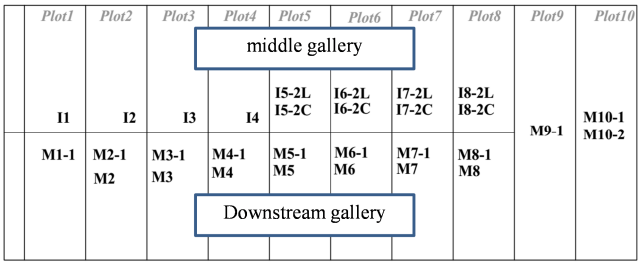

Figure 2. *Position of the piezometers at the Songloulou water intake dam.*

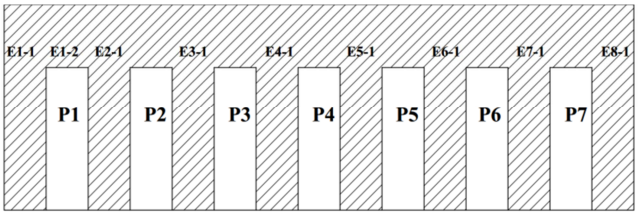

Figure 3. *Position of the piezometers at the Songloulou evacuator dam.*

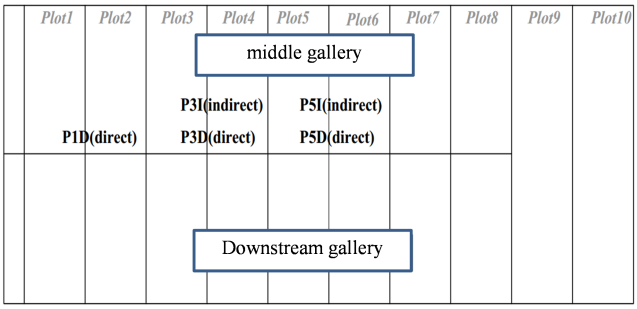

Figure 4. *Position of the pendulums at the intake dam of the Songloulou hydroelectric development.*

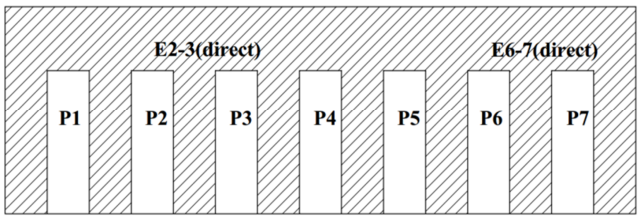

Figure 5. *Position of the pendulums at the Spillway Dam of the Songloulou hydroelectric facility.*

The displacements measured on either side of the dam and the uplifts measured in the dams at the level of the concrete-rock contact and upstream are generally strongly influenced by the upstream coast. By applying the model (HST Hydrostatic Season Time) the calculated hydrostatic effect is an average effect which is identical regardless of the season. A more detailed analysis of the data shows that this hydrostatic effect is not the same in the dry season and in the wet season. The zone in which the uplifts are measured is a "fractured zone" and its state of fracturing depends on the position of the dam: in the dry season, with the expansion of the concrete, the dam assumes an upstream position and the cracking at the substructure tends to close. Conversely, in the rainy season, with the contraction of the concrete, the dam is

positioned further downstream and cracking at the upstream toe is greater. This effect is not included in the HST model which considers a hydrostatic effect averaged over all the seasons. To overcome this drawback, we use in this paper neural networks which have the ability to create differentiated hydrostatic effects according to the seasons. On the same principle, the seasonal effect is not necessarily identical to RN (normal retention) or to empty retention. A neural network will have the ability to capture this cross-link between the season and the odds.

3.1. Calibration and Operation of the Fuzzy Neuron Tool

For the realization of our network, we use the Matlab software [35], in the applications (APPS) that this software offers, in the "CONTROL SYSTEM DESIGN AND ANALYSIS" part, the "Neuro-fuzzy Designer" application, the main tool of our programming. For our model (Figure 6) we will use three explanatory variables as input: the level of the reservoir (z), the season (s) and the time (t). The output will represent the estimated behavior of the piezometer.

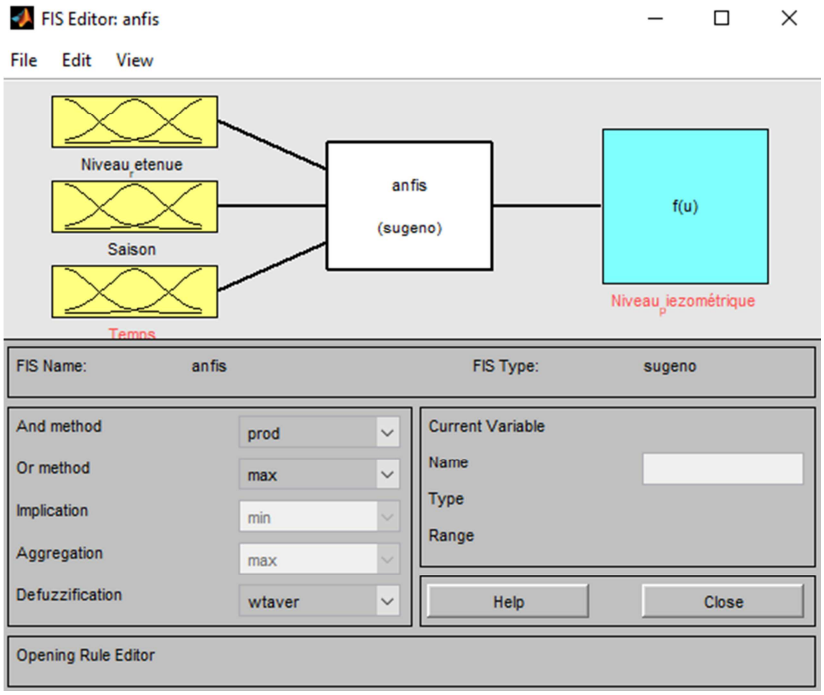

a)

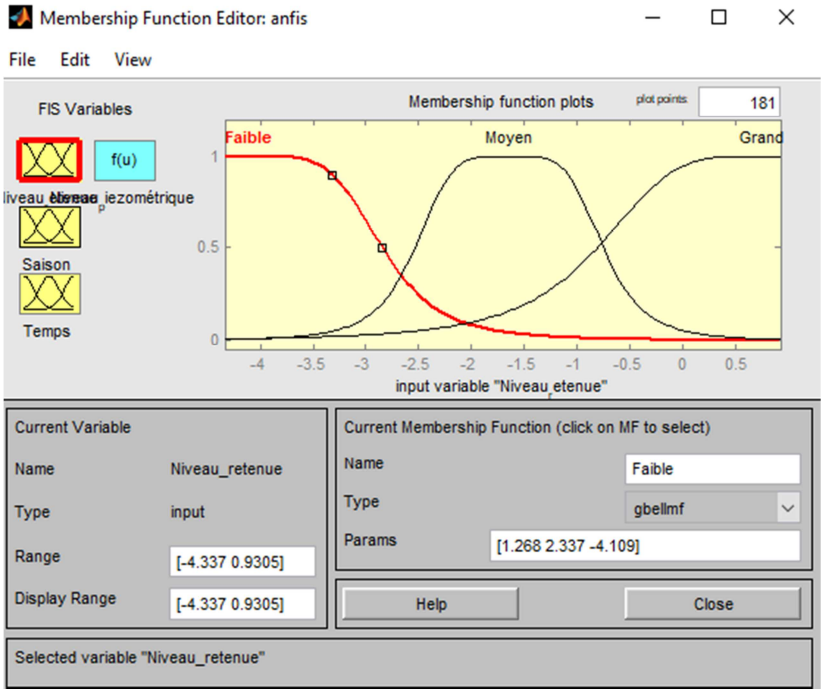

b)

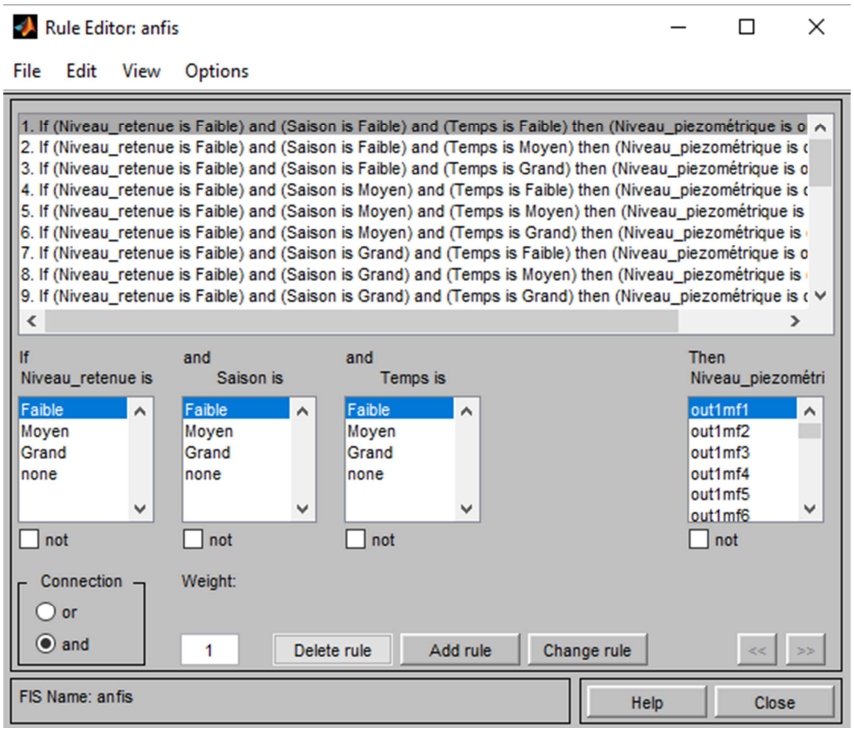

c)

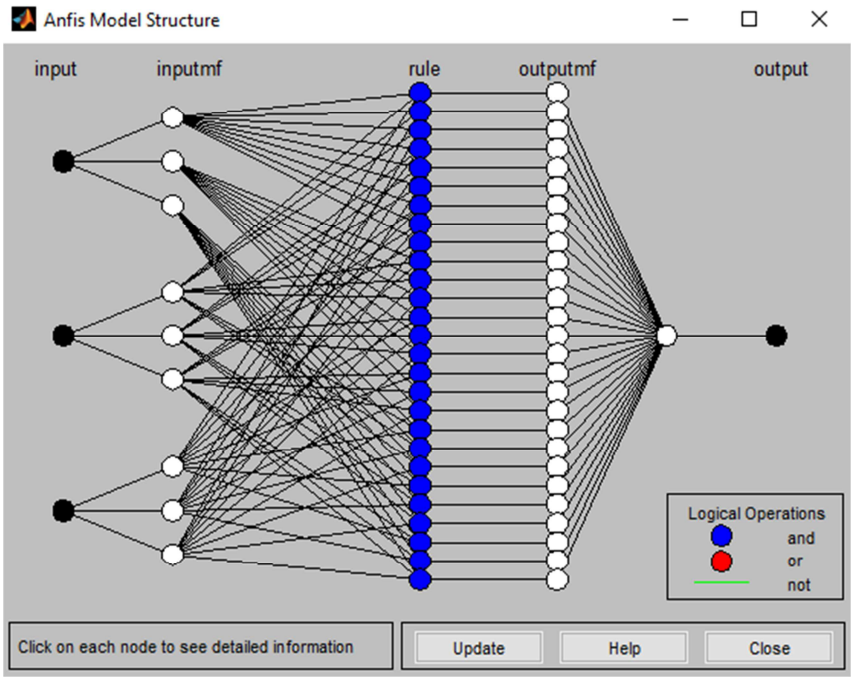

d)

Figure 6. *Main tool of our programming: a) Determination of inputs and outputs. b) Variable membership functions. c) Writing rules in Matlab. d) Architecture of the ANFIS network.*

3.2. Network of the Parameters of the Fuzzy Neuron Method

All the details used in this work are developed in the scientific and technical documents published by the referenced authors [9, 26, 28-34].

Table 1 describes the neural network developed, it can be interpreted as follows: the Number of entries represents the number of explanatory variables which are here the level of the reservoir, the season and the time; the membership function is the function chosen to describe the phenomenon, given that the curves are not affine and go jagged, we have opted for the Bellshape function. The type of inference chosen in this study is Sugeno because the membership functions are precise values.

Table 1. *Presentation of the piezometer network.*

Number of entry	3
Membership functions	Bellshape, 3 for entrance
T-norm	Product
Type of inference	Sugeno
Number of neuron	67
Number of premise parameters	27= 3*3
Number of consequent parameters	108=27*4
Total number of parameters	135
Total number of training data	132
Learning algorithm	Gradient backpropagation and least squares method
Number of fuzzy rulers	27

4. Analysis of the HST Model and That of the Fuzzy Neural Network on the Songloulou Hydroelectric Dam

4.1. Intake Dam: Exploitation of Piezometric Data

4.1.1. Use of Piezometer I1 Data

Table 2 presents a summary of the new values of the membership function parameters of the piezometer I1 using Bellshape type membership functions. From the ANFIS model (Adaptive Neuro Fuzzy Inference System) the results of the piezometer I1 are given.

Table 2. *Final parameters of the membership functions of the piezometer I1.*

final function	weak			average			hight		
	ai	bi	Ci	ai	bi	ci	ai	bi	ci
level	1.0947	2.3585	-4.2974	0.4738	2.5804	-1.3234	1.8114	1.6035	0.9052
season	1.5757	1.182	-0.2852	1.1378	3.3772	2.2213	1.6374	3.3772	2.2213
time	2.7784	2.3521	0.2099	1.5173	3.8164	5.2822	3.8372	3.3488	8.9724

After training and developing the new parameters, we determined the different parameters n_i, s_i, t_i and b_i according to the established rules (Table 3), which represent the coefficients of the final parameters of the model used.

Table 3. *Coefficient of final parameters.*

function	Parameters				
	Coefficient of the variable level retained: n	of the variable Season: s	of the variable Time: t	b	w_i
$out1\_f_1$	-66.86201	14.66457	103.99512	28.52094	0.000718018
$out1\_f_2$	-13.67075	80.16198	118.95478	32.38700	0.002916573
$out1\_f_3$	26.12609	52.01292	37.84743	10.14450	0.003682125
$out1\_f_4$	-60.08609	34.65492	62.39650	16.05303	0.000398601
$out1\_f_5$	-21.82759	32.43701	58.24856	16.96844	0.001619106
$out1\_f_6$	12.12196	40.67423	55.84260	10.86692	0.002044095
$out1\_f_7$	-1.22492	-20.75657	-8.41647	-0.06685	0.000799131
$out1\_f_8$	-8.96193	4.18536	2.33630	9.01214	0.003246051
$out1\_f_9$	-12.70787	-0.77933	43.79042	7.22182	0.004098085
$out1\_f_{10}$	-78.95026	181.33469	71.64195	215.4254	0.000748617
$out1\_f_{11}$	3.25957	-29.03033	125.71012	15.11556	0.003040863
$out1\_f_{12}$	13.82312	55.21798	37.42386	-19.59825	0.00383904
$out1\_f_{13}$	2.05086	-124.93501	191.85175	99.11219	0.000415587
$out1\_f_{14}$	34.83082	72.43588	89.51021	88.88520	0.001688105
$out1\_f_{15}$	-77.30770	-142.24788	55.84266	16.87389	0.002131204
$out1\_f_{16}$	-12.24695	50.66410	115.60437	20.02558	0.000833186
$out1\_f_{17}$	-8.64564	-18.49168	109.95610	72.26042	0.003384382
$out1\_f_{18}$	46.76177	18.06850	52.46139	27.78286	0.004272726
$out1\_f_{19}$	-12.06337	3.22211	0.89449	499.6492	0.03531372
$out1\_f_{20}$	-3.19847	-4.73258	-1.87640	508.2304	0.14344351
$out1\_f_{21}$	12.88944	13.54366	-1.47723	497.2053	0.181095058
$out1\_f_{22}$	-1.21297	-0.77610	-0.44070	502.0313	0.019604057
$out1\_f_{23}$	2.44147	0.11472	0.72269	496.5514	0.079631225
$out1\_f_{24}$	-6.96780	-0.78891	0.40666	494.3632	0.100533104
$out1\_f_{25}$	0.56275	0.09870	-0.17007	497.8733	0.039303016
$out1\_f_{26}$	-0.85591	-0.28260	0.00612	502.0062	0.159647936
$out1\_f_{27}$	0.04226	0.58579	-0.05504	492.7806	0.201552878

To evaluate the evolution of the level of the piezometer I1, the explanatory variable "Level of the reservoir" which is the variable which seems the most interesting at first sight was fixed, we use as second variable the Season and then the Time (duration of the geotechnical structure). Figure 7-a shows that the season acts sinusoidally on the level of piezometer I1. This reflects an almost constant behavior of the ground. The lower the water level in the dam, the lower the pressure in the ground. But at certain times, due to the variability of the seasons over time, there are slight differences at the level of the coast of the piezometer I1. This effect proves that the soil reacts well to climatic hazards. The effects of water level and time on the level of this piezometer are highlighted in Figure 7-b. It can be seen that the water level in the dam significantly influences the piezometry. This influence does not decrease over time, which a priori is not reassuring for the structure. Over time, this should decrease due to the consolidation of the soil which should have led to the removal of pore pressures.

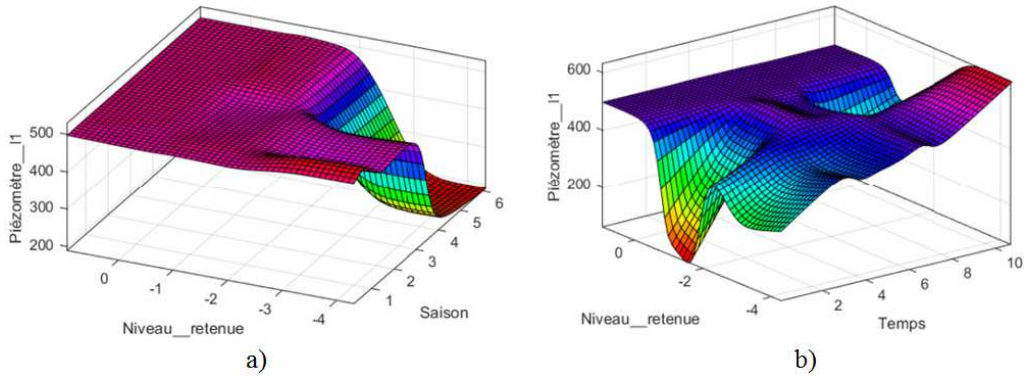

Figure 7. *Evolution of the level of piezometer 1: a) depending on the water level and the season; b) depending on the water level and the weather (lifetime of the structure).*

Analysis of the results: Validation of the model and comparison with the HST method.

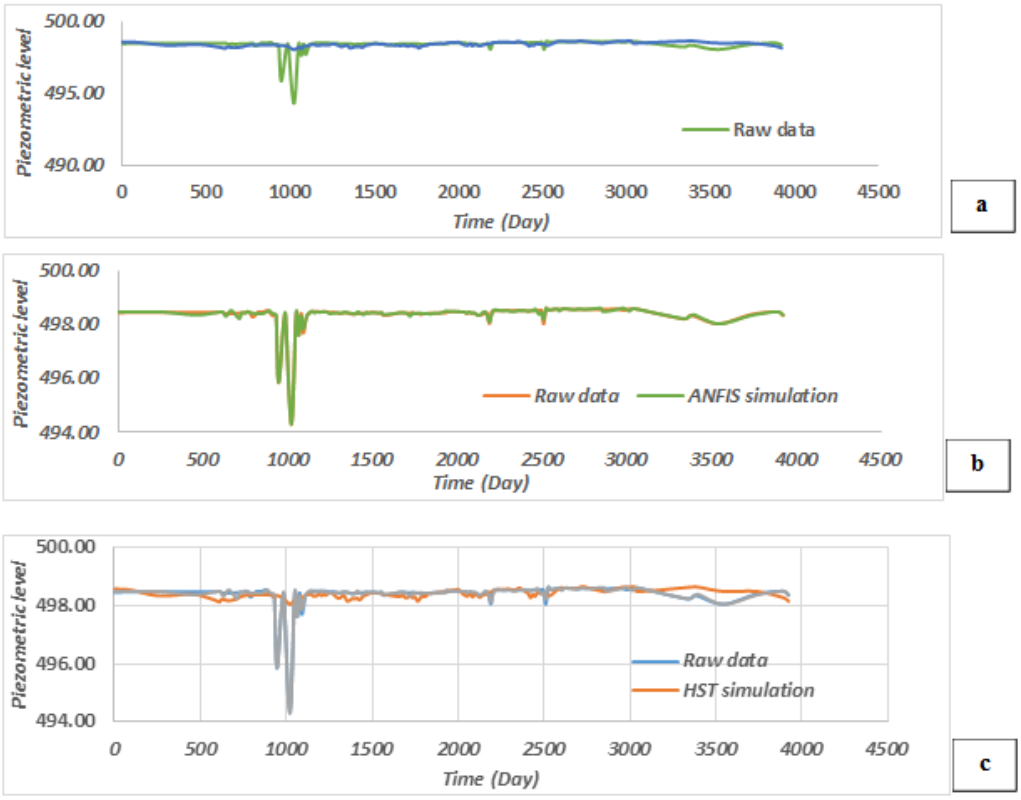

Figure 8. *Comparison of the different behavior models of the I1 piezometer.*

Figure 8 indeed shows that the ANFIS model is more compatible with the data observed on the I1 piezometer than the HST model (Figure 8-a) which is unable to predict the peaks. There is indeed a difference between the two models (figure 8-c).

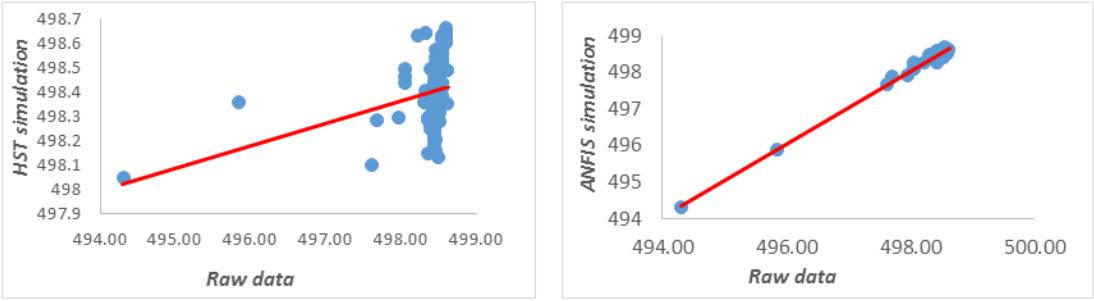

Figure 9. *Comparison between the real data and the simulated data of the piezometer I1.*

It can be seen that the correlation in the case of the ANFIS model is good and centered around a straight line, while in the HST model the values are quite scattered (Figure 9). The ANFIS model better represents the real data. Table 4 presents here the criteria for comparing the different models. It can be seen from Table 4 that the evaluation of the phenomenon based on the fuzzy neuron model describes well the behavior of the piezometer I1, because the mean squared error (MSE) is low and the correlation coefficient high compared to the HST model. This adequacy is justified by the fact that the model makes it possible to highlight the cross-relationships existing between the different explanatory variables. A shortcoming that the conventional model (HST) has due to the assumption of superposition of the said variables. The MAPE criterion (Mean Absolute Percentage Error) is low, which proves that the system does not correctly predict the behavior of the piezometer I1 in the short term. D and Dα are parameters of the Kolmogorov-Smirnov test.

Table 4. *Comparison of HST and ANFIS.*

	Model	***HST***	***ANFIS***
	MSE	0.18097573	0.00249069
	NASH	-8.8586626	0.98734384
	R	9.21%	98.75%
	MAPE	0.04491726	0.00829865
Kolmogorov-	D	0.00015226	0.00018488
Smirnov	Dα	0.11837281	0.11837281

Assumptions of the Kolmogorov-Smirnov Test:

H0: the simulated values are not significantly different from the real values,

H1: the simulated values are significantly different from the real values.

The principle of the test consists in calculating the cumulative distribution of the theoretical proportions and comparing it with those observed. The test statistic is considered to be: D, the maximum difference in absolute value between the observed cumulative proportions and the simulated cumulative proportions.

$$D = max\|PcO - PcT\|$$

For the piezometer I_1 (ANFIS model),

$$D = 0.00018488$$

The critical value Dα at threshold α = 5% for a sample of size n (n > 35) is given by: $D_\alpha = \frac{1.36}{\sqrt{n}}$ either $D_\alpha =$ 0.11837281

Table 5. *Performance evaluation of the different prediction models on all the piezometers.*

Piezometer	***model***		***HST***	***ANFIS***
	MSE		*1.01654506*	*0.0391054*
	NASH		*0.00876777*	*0.98033811*
	R		*50.22%*	*98.09%*
E1-1	*MAPE*		0.21546735	0.03328576
	Kolmogorov-	*D*	0.00022238	0.00036481
	Smirnov	*Dα*	0.11837281	0.11837281
	MSE		*0.18097573*	*0.00249069*
	NASH		*-8.8586626*	*0.98734384*
	R		*9.21%*	*98.75%*
I1	*MAPE*		0.04491726	0.00829865
	Kolmogorov-	*D*	0.00015226	0.00018488
	Smirnov	*Dα*	0.11837281	0.11837281
	MSE		*0.7199511*	*0.00722191*
	NASH		*-1.9900762*	*0.99242235*
	R		*25.06%*	*99.25%*
I2	*MAPE*		0.1877615	0.01529493
	Kolmogorov-	*D*	1.60E-04	3.39E-04
	Smirnov	*Dα*	0.11837281	0.11837281
	MSE		*0.08864675*	*0.00649858*
	NASH		*-5.6616545*	*0.93187339*
	R		*13.05%*	*93.63%*
I3	*MAPE*		0.03171359	0.00885452
	Kolmogorov-	*D*	0.00013798	0.00015548
	Smirnov	*Dα*	0.11837281	0.11837281
	MSE		*0.00873718*	*0.0031229*
	NASH		*-0.1914663*	*0.7567704*
	R		*45.63%*	*80.57%*
I8-2L	*MAPE*		0.01801691	0.0087981
	Kolmogorov-	*D*	1.35E-04	1.34E-04
	Smirnov	*Dα*	0.11837281	0.1183728
	MSE		*0.26905319*	*0.0022615*
	NASH		*-8.8586626*	*0.9873438*
	R		*8.87%*	*99.23%*
M1-1	*MAPE*		0.05758224	0.0081616
	Kolmogorov-	*D*	0.00013036	0.0001492
	Smirnov	*Dα*	0.11837281	0.1183728
	MSE		*0.06852541*	*0.00252257*
	NASH		*-3.2512176*	*0.96926997*
	R		*19.04%*	*97.02%*
I4	*MAPE*		0.03758204	0.00821245
	Kolmogorov-	*D*	5.47E-05	6.18E-05
	Smirnov	*Dα*	0.11837281	0.11837281
	MSE		*6.9733032*	*0.00297777*
	NASH		*-8.9315753*	*0.99961191*
	R		*9.15%*	*99.96%*
I5-2L	*MAPE*		0.31130267	0.01013079
	Kolmogorov-	*D*	0.00048475	0.00066052
	Smirnov	*Dα*	0.11837281	0.11837281

Piezometer	*model*		*HST*	*ANFIS*
I6-2L	*MSE*		*0.01470121*	*0.00230562*
	NASH		*-5.6992833*	*0.84326898*
	R		*12.99%*	*86.35%*
	MAPE		0.02440705	0.00847497
	Kolmogorov-	*D*	7.44E-05	9.49E-05
	Smirnov	*Dα*	0.11837281	0.11837281
I7-2L	*MSE*		*0.030974*	*0.00658386*
	NASH		*-5.6992833*	*0.84326898*
	R		*27.58%*	*84.61%*
	MAPE		-1.62570427	0.81736629
	Kolmogorov-	*D*	1.44E-04	1.55E-04
	Smirnov	*Dα*	0.11837281	0.11837281
M6-2	*MSE*		*0.04371014*	*0.00889755*
	NASH		*-7.0579013*	*0.78665187*
	R		*11.04%*	*81.89%*
	MAPE		0.02065605	0.01549152
	Kolmogorov-	*D*	1.27E-04	1.39E-04
	Smirnov	*Dα*	0.11837281	0.11837281
M7-2	*MSE*		*0.01880582*	*0.00463144*
	NASH		*-0.595434*	*0.82019766*
	R		*38.53%*	*84.86%*
	MAPE		0.02345939	0.0096185
	Kolmogorov-	*D*	1.56E-04	1.52E-04
	Smirnov	*Dα*	0.11837281	0.11837281
M2-1	*MSE*		*0.7199511*	*0.00722191*
	NASH		*-1.9900762*	*0.99242235*
	R		*25.06%*	*99.25%*
	MAPE		0.1877615	0.01529493
	Kolmogorov-	*D*	1.60E-04	3.39E-04
	Smirnov	*Dα*	0.11837281	0.11837281
M3-1	*MSE*		*0.2891059*	*0.0034373*
	NASH		*-3.2128611*	*0.99029053*
	R		*19.18%*	*99.04%*
	MAPE		0.08921857	0.0097318
	Kolmogorov-	*D*	1.13E-04	1.60E-04
	Smirnov	*Dα*	0.11837281	0.11837281
M4-1	*MSE*		*0.02583915*	*0.00258702*
	NASH		*-0.4467653*	*0.9368043*
	R		*40.87%*	*94.08%*
	MAPE		0.0346867	0.00819494
	Kolmogorov-	*D*	8.47E-05	8.69E-05
	Smirnov	*Dα*	0.11837281	0.11837281
M5-1	*MSE*		*0.05308272*	*0.00940327*
	NASH		*0.5238724*	*0.93941527*
	R		*67.74%*	*94.29%*
	MAPE		0.0367271	0.01289637
	Kolmogorov-	*D*	0.00032319	0.00030788
	Smirnov	*Dα*	0.11837281	0.11837281
M5-2	*MSE*		*0.03553419*	*0.00063743*
	NASH		*-0.4264033*	*0.98932728*
	R		*41.21%*	*98.95%*
	MAPE		0.21546735	0.03328576
	Kolmogorov-	*D*	0.00022238	0.00036481
	Smirnov	*Dα*	0.11837281	0.11837281
M8-2	*MSE*		*0.01880582*	*0.00463144*
	NASH		*-0.595434*	*0.82019766*
	R		*38.53%*	*84.86%*
	MAPE		0.02345939	0.0096185
	Kolmogorov-	*D*	1.56E-04	1.52E-04
	Smirnov	*Dα*	0.11837281	0.11837281
M8-1	*MSE*		*0.00460024*	*0.01644953*
	NASH		*-0.118744*	*0.82498519*
	R		*47.20%*	*85.23%*
	MAPE		0.02308931	0.01074947
	Kolmogorov-	*D*	1.48E-04	1.34E-04
	Smirnov	*Dα*	0.11837281	0.11837281

Piezometer	*model*		*HST*	*ANFIS*
M9-1	*MSE*		*0.97957829*	*0.17354932*
	NASH		*-0.0800774*	*0.89717252*
	R		*48.08%*	*90.80%*
	MAPE		0.19712565	0.0621059
	Kolmogorov-	*D*	1.67E-04	2.22E-04
	Smirnov	*Dα*	0.11837281	0.11837281
M10-1	*MSE*		*1.60972866*	*0.05971698*
	NASH		*0.00337126*	*0.9809826*
	R		*50.08%*	*98.15%*
	MAPE		0.26691034	0.04057676
	Kolmogorov-	*D*	3.26E-04	4.17E-04
	Smirnov	*Dα*	0.11837281	0.11837281
M10-2	*MSE*		*0.88717832*	*0.03048639*
	NASH		*-0.0773726*	*0.98172326*
	R		*48.14%*	*98.22%*
	MAPE		0.19400747	0.02962152
	Kolmogorov-	*D*	2.83E-04	4.20E-04
	Smirnov	*Dα*	0.11837281	0.11837281

We see D < Dα so the hypothesis H0 is accepted. Then the simulated values of the ANFIS model are not significantly different from the real values. The same analysis process is carried out on all the piezometers. The summary in table 5 presents the different criteria for assessing the model as well as the graphic representations of the piezometers used. To better appreciate the efficiency of the fuzzy neuron model, a comparison is made with the HST model corresponding to each exploitable piezometer. Table 5 presents a summary of the predictive indicators of each model according to the data from the various piezometers of the dam. Upon analysis of the correlation indicators presented in Table 5, it clearly appears that the ANFIS model correctly predicts the phenomenon studied with correlation coefficients R greater than 80% on the data from all the piezometers.

4.1.2. Piezometer M1-1

Figure 10-b shows us that the ANFIS model closely approximates the behavior of the M1-1 piezometer over the entire duration of the measurement. The basic model (HST) tends to generalize the system (figure 10-a), and approximates the behavior of the piezometer more or less well until 2015 when the peaks become larger and larger, from then on the HST model does not can't keep up anymore. There are then notable differences between the two models (figure 10-c). Figure 11-b shows us the effect of water level and time on the level of piezometer M1-1. It can be seen that the water level in the dam significantly influences the piezometry. Over time, this should decrease due to the consolidation of the soil, which should have led to the removal of the voids. It is noted in Figure 11-a, that the season acts in a sinusoidal way on the coast of the piezometer M1-1. This reflects an almost constant behavior of the ground. The lower the water level in the dam, the lower the pressure in the ground. But at certain times, due to the variability of the seasons over time, there are slight differences at the level of the M1-1 piezometer level. This proves that the soil reacts well to climatic hazards.

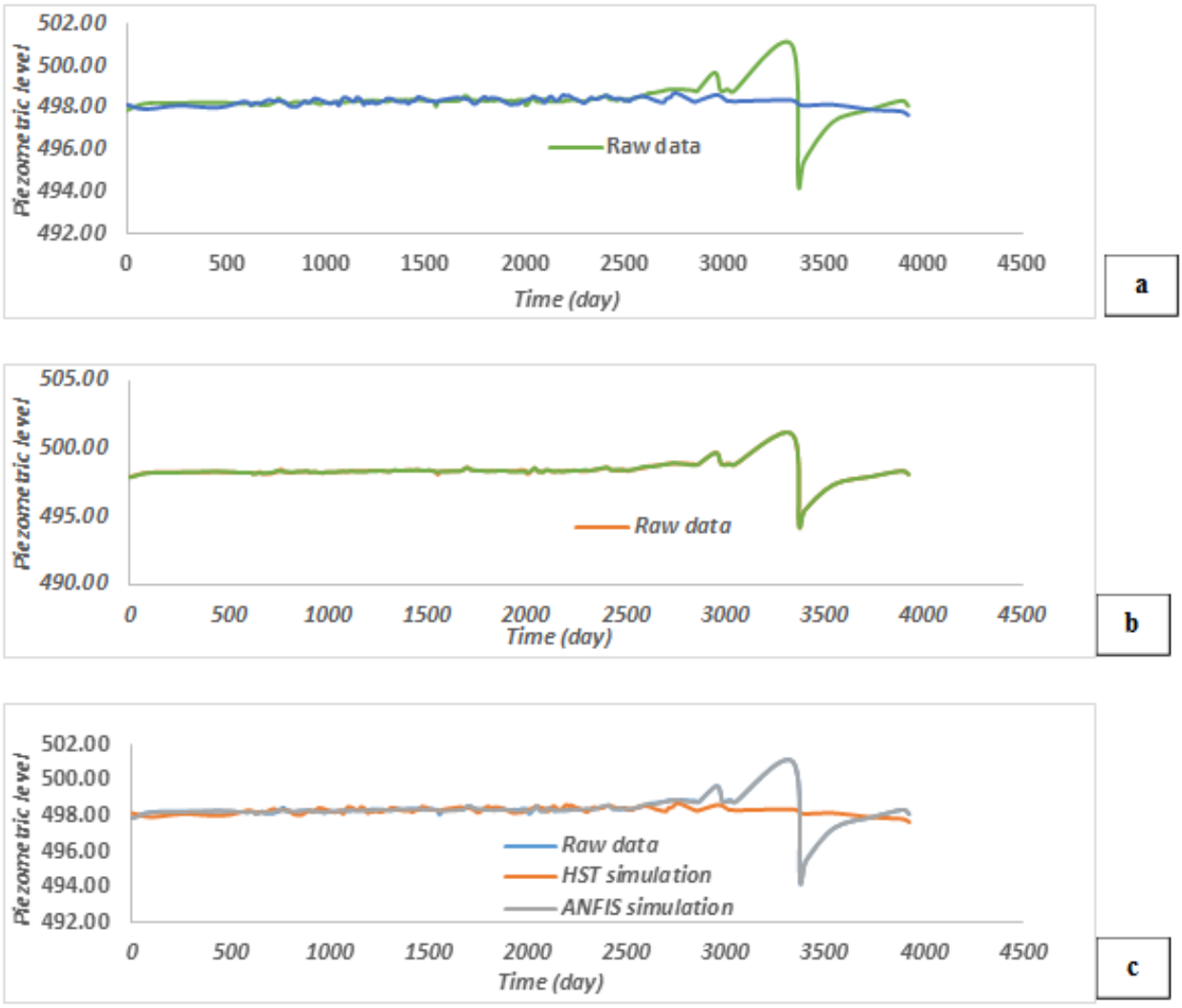

Figure 10. *Comparison of the different behavior models of the M1-1 piezometer.*

It is also interesting to note that in the neighborhoods of the RN (Normal Reservoir), the piezometric level does not change almost whatever the season, this shows the preponderance of the influence once again of the level of the reservoir with respect to the season.

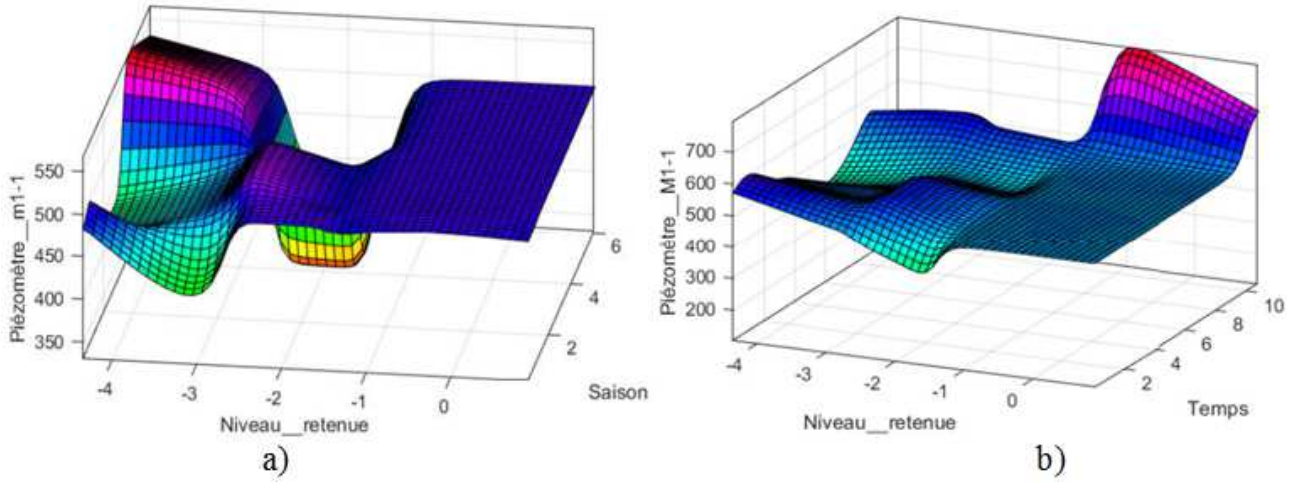

Figure 11. *Evolution of the piezometer level: a) M1-1 as a function of the water level and the season; b) M1_1 depending on the water level and time- M1_1 depending on the water level and time (lifetime of the structure).*

4.1.3. Piezometer I2

Figure 12. *Comparison of the different behavior models of the I2 piezometer.*

Figure 12-b shows us that the ANFIS model closely approximates the behavior of the M1-1 piezometer over the entire duration of the measurement. The basic model (HST) tends to generalize the system (figure 12-a), and more or less approaches the behavior of the piezometer except when we have peaks like in 2010 or between 2016 and 2019.

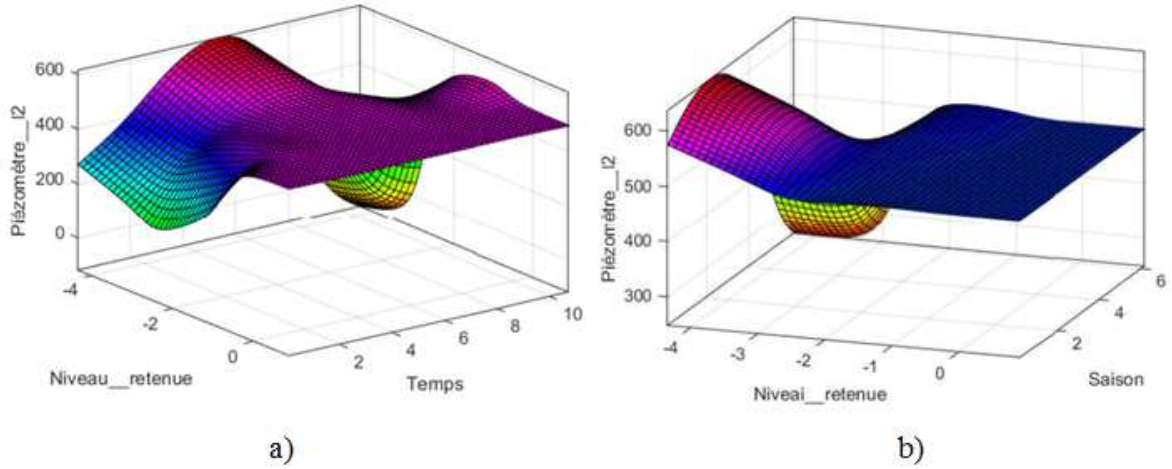

Figure 13. *Evolution of the I2 piezometer level: a) Depending on the water level and time; b) According to the coast of the water and the season.*

Figure 13-a shows us the influence of the level of the reservoir and time on the level of the piezometer I2, we notice immediately that as for the previous piezometers, the level of the reservoir has a significant influence on the piezometric level, in fact, we notice that around 0 the piezometric level hardly changes regardless of the time, yet logic would dictate that the consolidation of the ground over time also leads to a decrease in the influence of the level over time. The figure 13-b shows us the influence of the level of the reservoir and the season on the level of the piezometer I2, we notice immediately that as for the previous piezometers, that the season remains mute compared to the level of the reservoir at the around the normal retention level, thus the level of the reservoir once again demonstrates the preponderance of its influence whatever the season, even ignoring the contraction and expansion of the concrete.

4.1.4. M3-1 Piezometer

Figure 14-b indeed shows that the ANFIS model is more compatible with the data observed on the M3-1 piezometer, indeed it manages to predict all the variations and follows the peaks very well unlike the HST model (figure 14-a) which has great difficulty in predicting the behavior of the piezometer at the level of sudden variations. There is indeed a difference between the two models (figure 14-c). One notices once again the domination of the influence of the piezometry in the neighborhoods of the normal reservoir, the weather hardly influences the level of the piezometry when the level of the reservoir is normal, which is almost always the case. We can underline the constant character whatever the season of the piezometric level in the vicinity of 0 which represents the average of the levels of reservoir, which shows the strong influence of the level of the reservoir compared to the season on the behavior of the piezometer M3-1 (Figure 15).

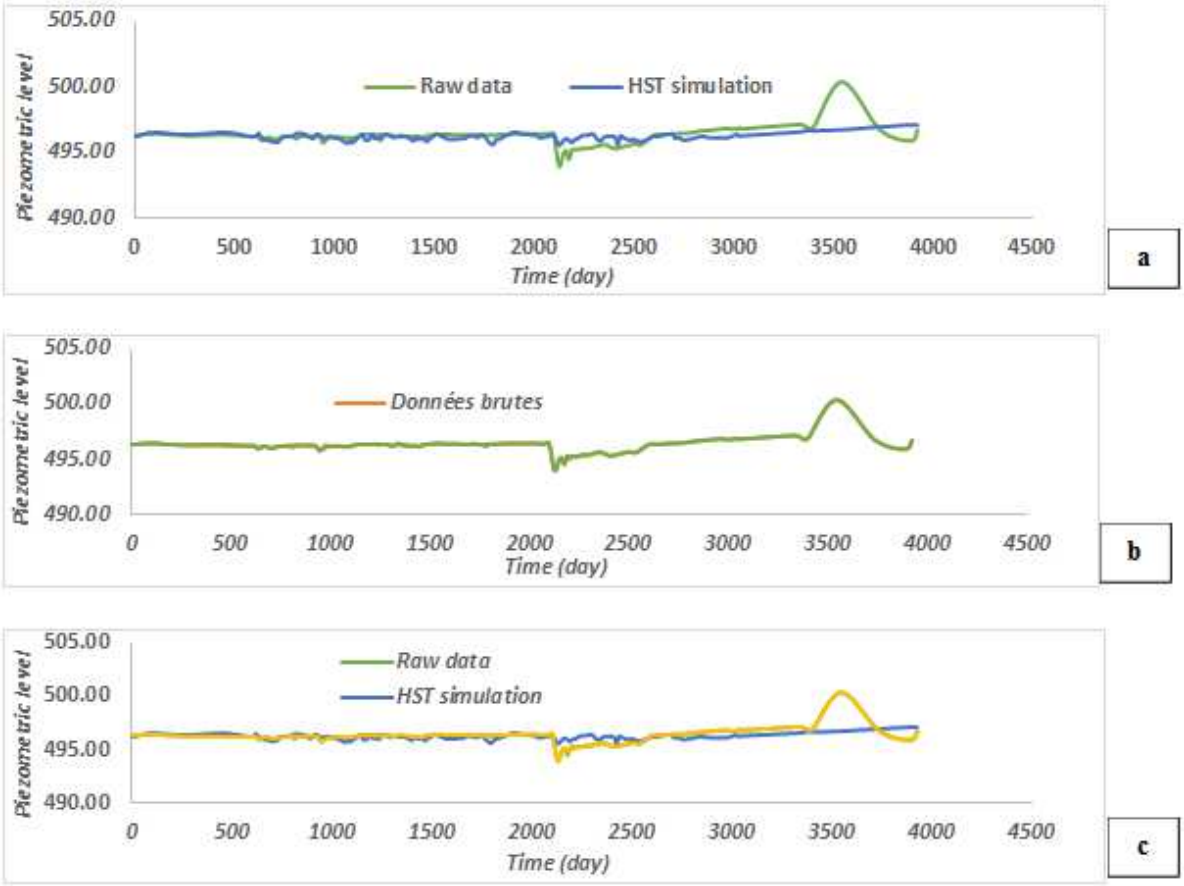

Figure 14. *Comparison of the different behavior models of the M3-1 piezometer.*

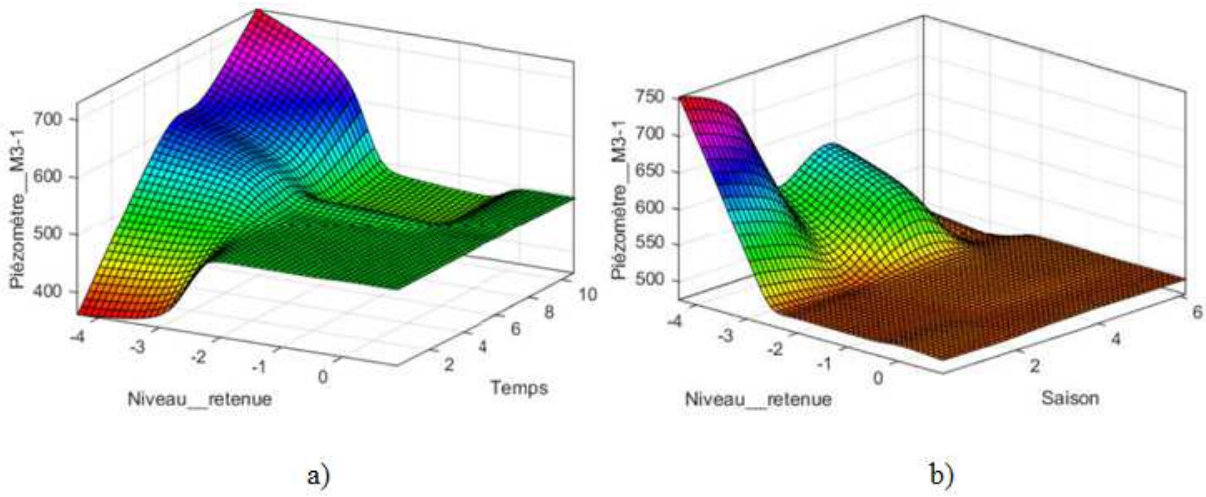

Figure 15. *Evolution of the elevation of the M3-1 piezometer: a) Depending on the elevation of the water and time (lifetime of the structure); b) According to the coast of the water and the season.*

4.1.5. Piezometer I3

One can immediately appreciate the power of the ANFIS model (figure 16-b) which apprehends the behavior of the piezometer very well and which faithfully predicts the results of the piezometer I3 compared to the HST model (figure 16-a) which always has a lot of difficulty to predict peaks, even if the prediction is acceptable. It is important to emphasize, apart from the strong influence of the reservoir level, that the piezometric levels remain much higher upstream than downstream, which testifies to the effectiveness of the sealing layer and the "non-communication" of water between the two galleries. The piezometric levels downstream remain lower than the levels upstream regardless of the season, which testifies to the effectiveness of the sealing layer. Note also here the strong influence of the level of the reservoir (Figure 17).

Figure 16. *Comparison of the different behavior models of the I3 piezometer.*

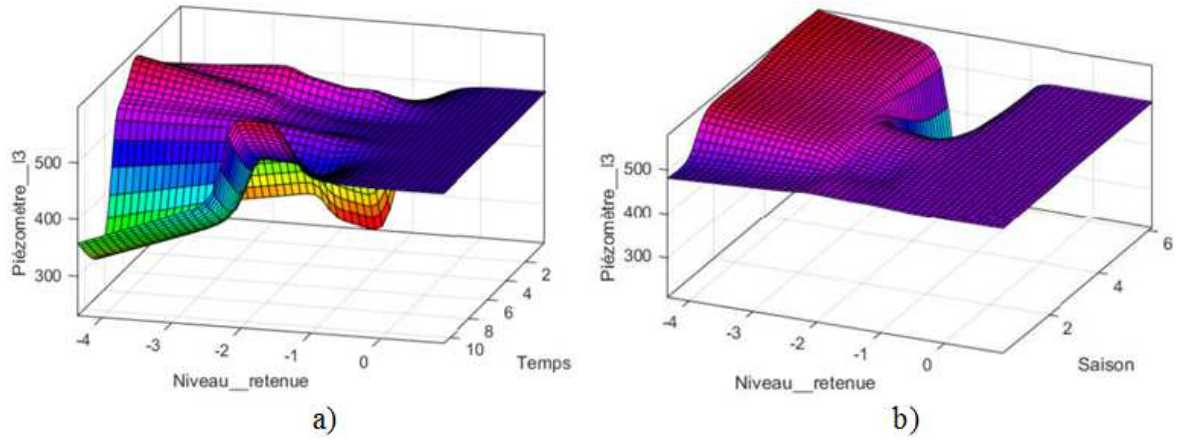

Figure 17. *Evolution of the elevation of the I3 piezometer: a) as a function of the elevation of the water and time (lifetime of the structure); b) depending on the water coast and the season.*

4.1.6. Piezometer M8-1

Figures 18 and 19 show the evolution of the water level in this piezometer as a function of time. Figure 18-b indeed shows that the ANFIS model is more compatible with the data observed on the M8-1 piezometer, indeed it manages to predict all the variations and follows the peaks very well unlike the HST model (figure 18-a) which has great difficulty in predicting the behavior of the piezometer at the level of sudden variations.

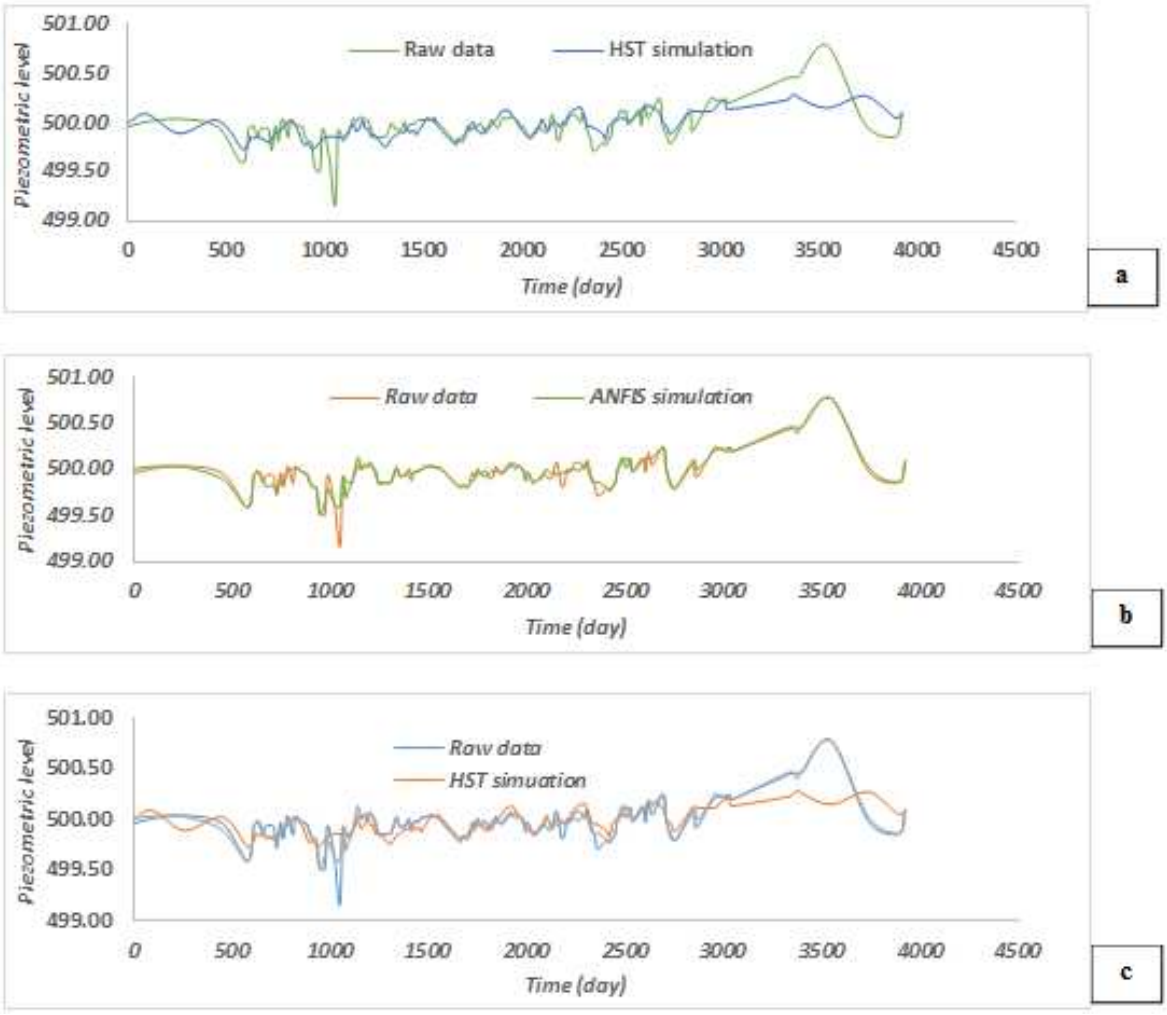

Figure 18. *Comparison of the different behavior models of the M8-1 piezometer.*

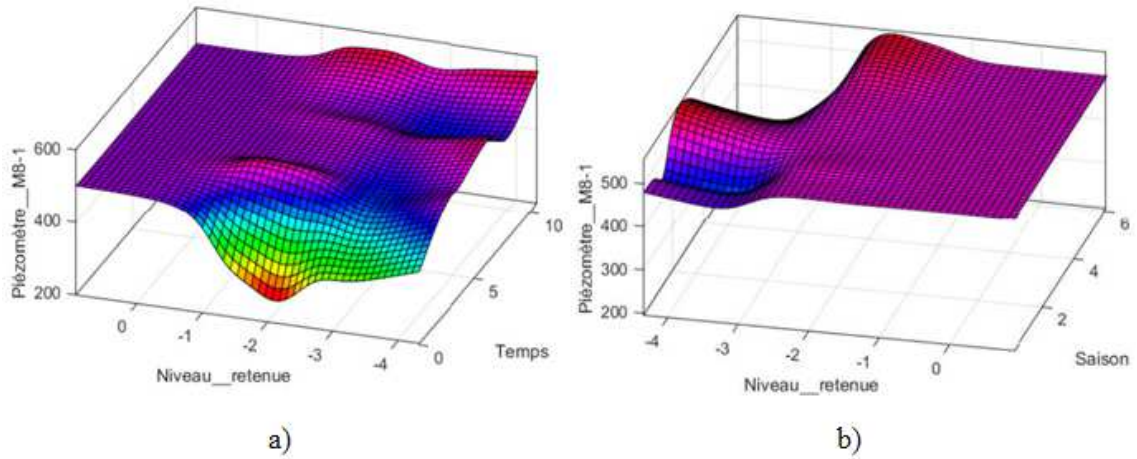

Figure 19. *Evolution of the elevation of the M8-1 piezometer: a) Depending on the elevation of the water and time (lifetime of the structure); b) According to the elevation of the water and the season.*

4.1.7. Piezometer I8-2L

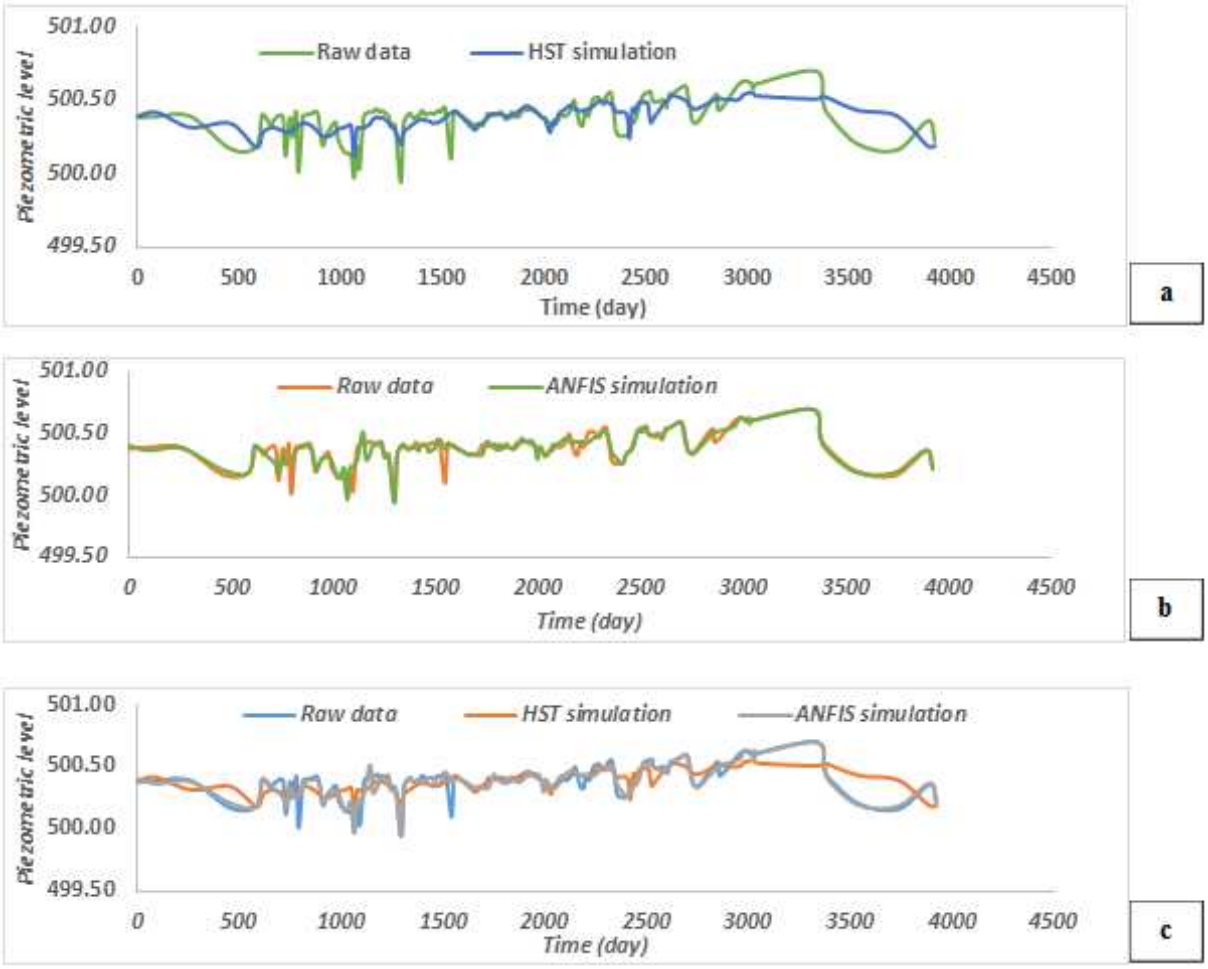

Figure 20. *Comparison of the different behavior models of the I8-2L piezometer.*

We see in figure 20 all the efficiency and power of the fuzzy neural network, this efficiency is verified on all the piezometers of the intake dam as can be seen on the piezometers above, for each of the piezometers, the model assimilates well the behavior of the devices. Figure 21-a shows us the influences of the reservoir level and time on the I8-2L piezometer level, as for all the other piezometers of the intake dam, the reservoir level has a significant influence on the piezometer level which hardly varies around 0.

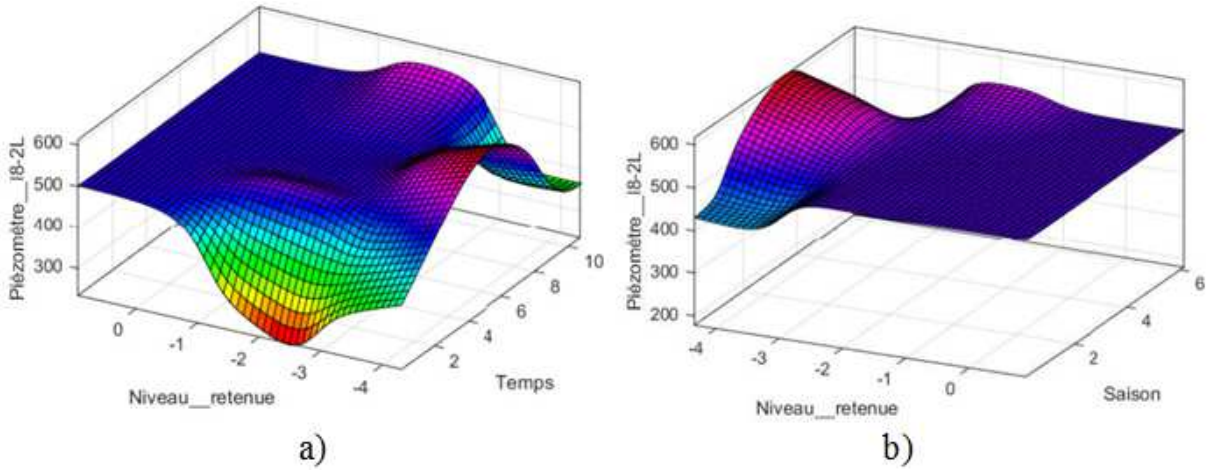

Figure 21. *Evolution of the elevation of the I8-2L piezometer: a) Depending on the elevation of the water and time (lifetime of the structure); b) According to the elevation of the water and the season.*

Figure 21-b shows the influences of the level of the reservoir and the season on the piezometer level I8-2L, as for all the other piezometers of the intake dam, the level of the reservoir has a significant influence on the piezometer level which hardly varies around 0.

4.1.8. M9-1 Piezometer

It can be seen that the two models apprehend the behavior of the M9-1 piezometer quite well when it operates in an almost linear manner (Figure 22-c). But the various observable peaks are well estimated by the ANFIS model (Figure 22-b) while the basic HST model (Figure 22-a) generalizes the behavior of the piezometry. Figure 23-a shows the influence of the level of the reservoir and of time on the piezometer level M9-1, unlike the other piezometers of the intake dam, the influence of the level of the reservoir drops significantly and a remarkable increase is observed the influence of time, with a piezometric level which increases with time.

Figure 23-b shows the influence of the reservoir level and the season on the M9-1 piezometer level, unlike the other piezometers of the intake dam, the influence of the reservoir level drops significantly and an increase remarkable the influence of the season through slight oscillations around the level of the normal reservoir.

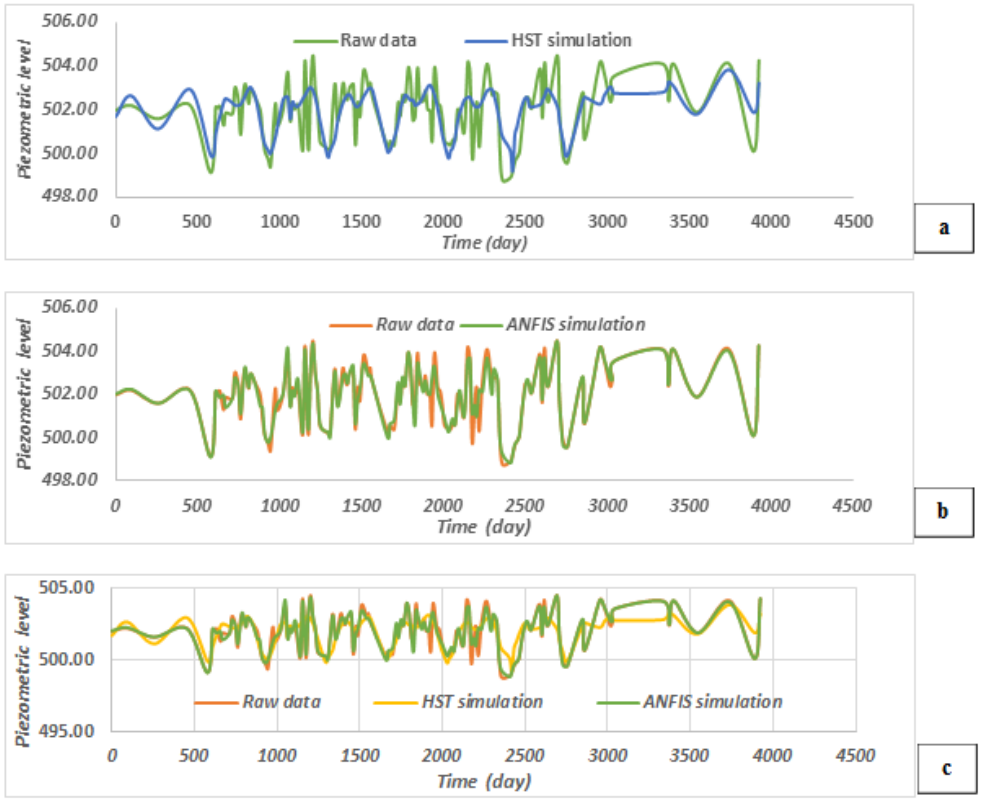

Figure 22. *Comparison of the different behavior models of the M9-1 piezometer.*

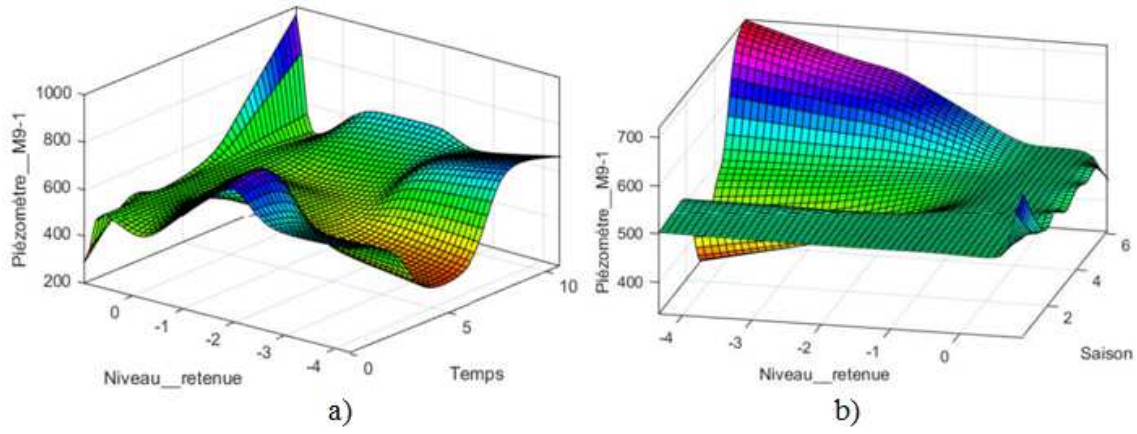

Figure 23. *Evolution of the M9-1 piezometer elevation; a) Depending on the coast of the water and the weather; b) According to the coast of the water and the season.*

4.1.9. Piezometer M10-1

It can be seen that the two models apprehend quite well the behavior of the M9-1 piezometer when it operates in an almost linear manner (Figure 24-c). But the various observable peaks are well estimated by the ANFIS model (Figure 24-b) while the basic HST model (Figure 24-a) generalizes the behavior of the piezometry.

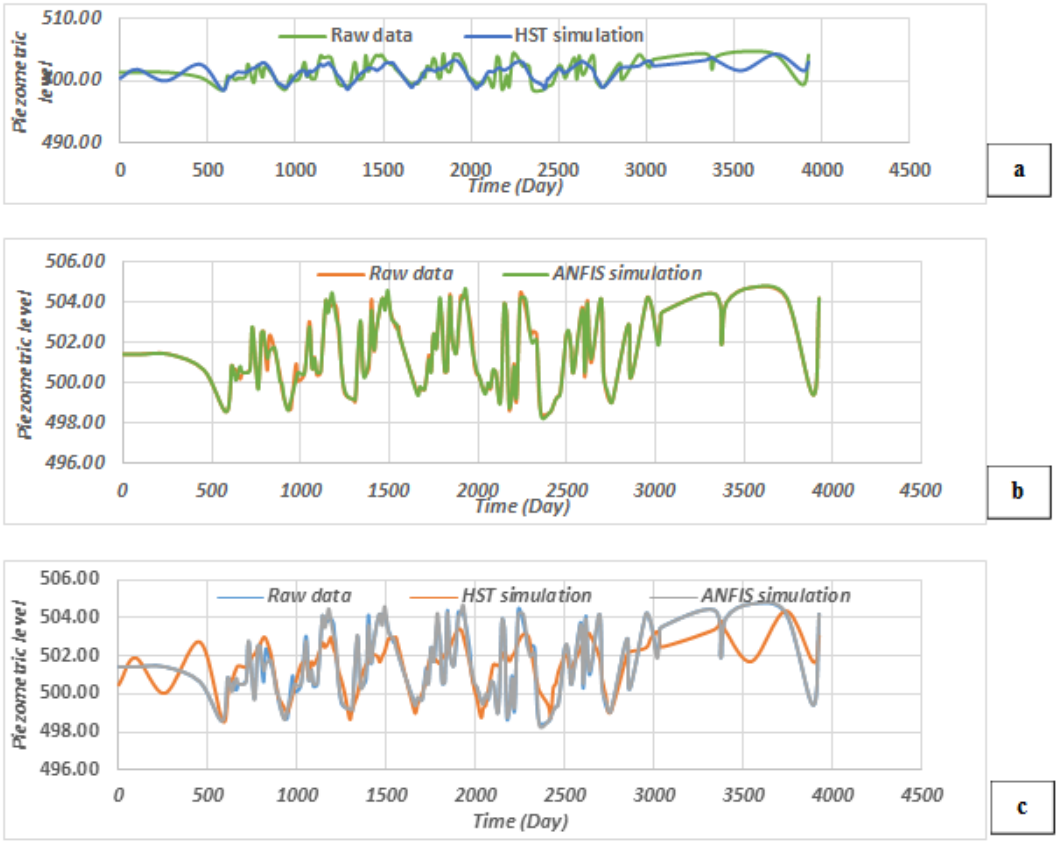

Figure 24. *Comparison of the different behavior models of the M10-1 piezometer.*

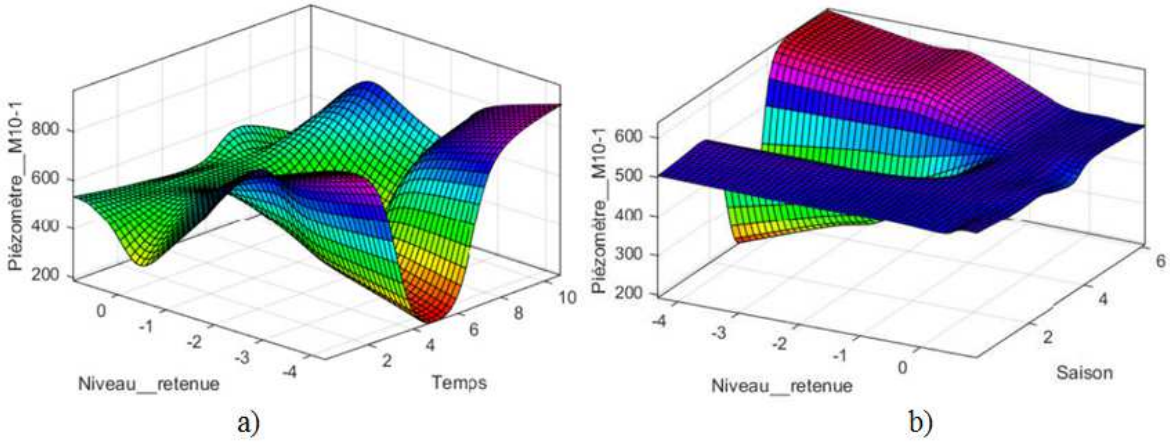

Figure 25. *Evolution of the M10-1 piezometer elevation; a) as a function of the water level and the weather (lifespan of the structure); b) According to the elevation of the water and the season.*

The figure 25-a, highlights the influences of the level of the reservoir and of time on the level piezometer M10-1, the influence of the level of the reservoir decreases significantly and one observes a remarkable increase in the influence of time better although on the M9-1 piezometer, with a piezometric level which increases with time, should we conclude that it is linked to the fact that we are approaching the spillway dam? Figure 25-b shows us the influences of the level of the reservoir and the season on the piezometer level M10-1, the influence of the level of the reservoir drops significantly and we observe a remarkable increase in the influence of the season through

slight oscillations around the normal restraint level. The behavior of the dam through all the piezometers is represented in the table 5. This behavior is typical on the ground of this region [36].

4.2. Spillway Dam: Exploitation of Piezometric Data

Figure 26-a indeed shows that the ANFIS model is more compatible with the data observed on the E1-1 piezometer than the HST model (Figure 26-b). There is indeed a difference between the two models (Figure 26-c). We can notice here, as already underlined on the M10-1 piezometer, a strong influence of time on the piezometric level, here it is confirmed, and the level of the reservoir is no longer as influential as on the intake dam.

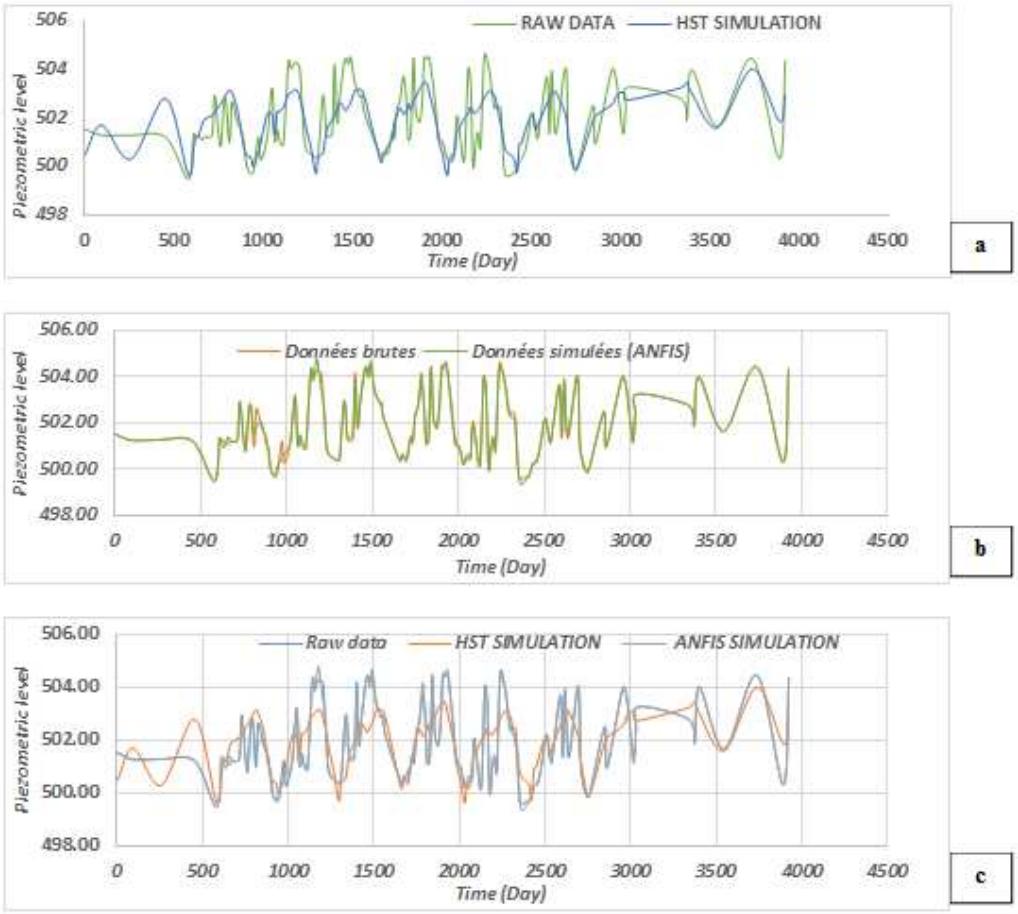

Figure 26. *Comparison of different piezometer behavior models E1-1.*

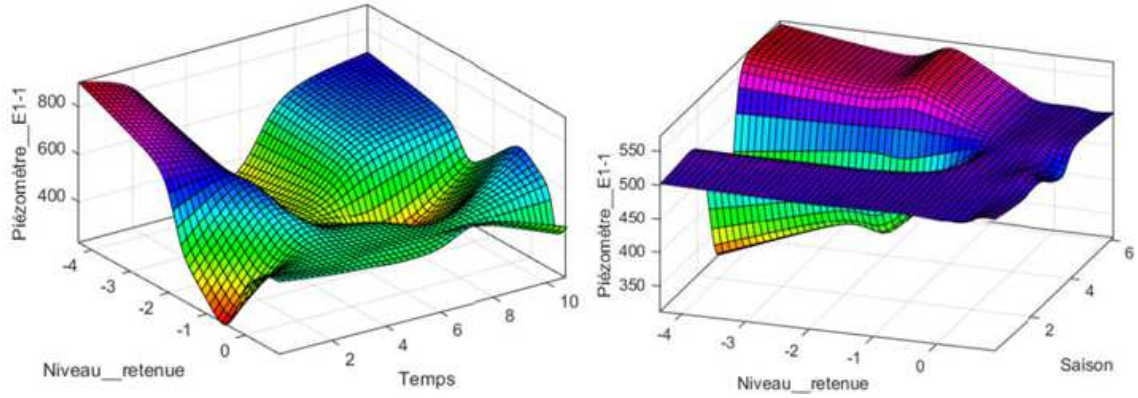

Figure 27. *Evolution of the elevation of the E1-1 piezometer as a function of the water elevation and time and depending on the water elevation and the season.*

Figure 27 shows the influences of the level of the reservoir and of the season on the piezometer level E1-1, the influence of the level of the reservoir decreases significantly and we observe a remarkable increase in the influence of the season through oscillations around the normal restraint level. The results presented in this part for the analysis of the under

pressures show that the water level in the dam significantly influences the piezometry at the level of the intake dam, we note at the level of this same dam that when we are at the normal reservoir level, the piezometric level hardly changes whatever the season or the weather, a priori this observation is worrying since the consolidation of the ground should logically reduce the influence of the level of the reservoir over time, but the lack of data from past periods and on the geology of the soil makes any conclusion premature; this being the case, it is nonetheless certain that the height of the reservoir has a preponderant influence on the piezometric level of the intake dam. From plot 9 (in the vicinity of the spillway dam) there is a significant increase in the influences of the season and the weather and a significant decrease in the influence of the level of the reservoir on the piezometry, and this analysis remains valid throughout. along the spillway dam, these fluctuations can be explained by the variations in activity on this dam according to the seasons (low water level, indeed during these periods, the spillways are open to evacuate the excess water in the dam, and are closed during periods of low flood); this dam is also the most affected by the Alkali-Granulate Reaction, which helps to observe strong seasonal variations.

4.3. Exploitation of Clock Data Displacement Measurements Were Made from 1997 to 2019

4.3.1. Displacements in the Pendulum P1D

After applying the HST and AFIS models to the raw data of the P1D pendulum, the results presented through figures 28 and 29 were obtained.

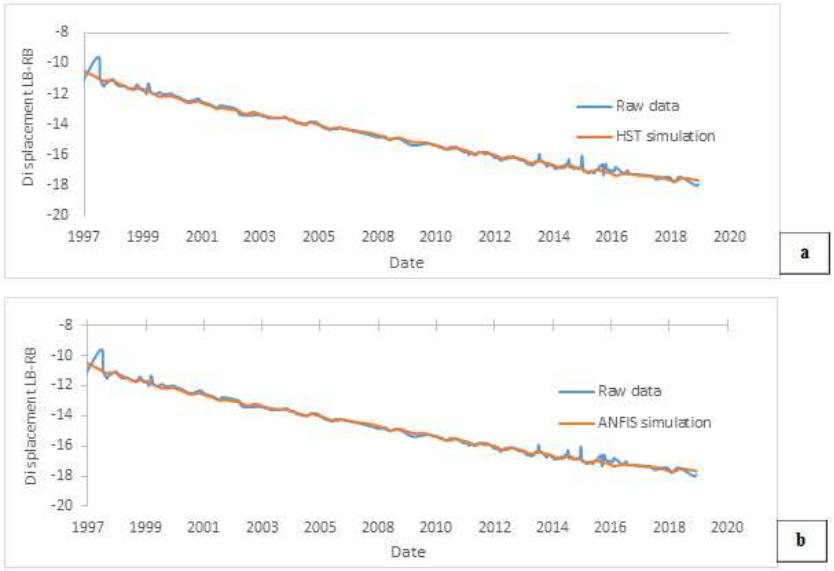

Figure 28. *Displacement (cm) Upstream-downstream pendulum P1D: (a) HST; (b) ANFIS.*

It can be seen that the two models apprehend quite well the behavior of the pendulum P1D when it operates in an almost linear manner. But the different observable peaks are well estimated by the ANFIS model (Figure 28-b) while the basic HST model (Figure 28-a) generalizes the behavior of the pendulum.

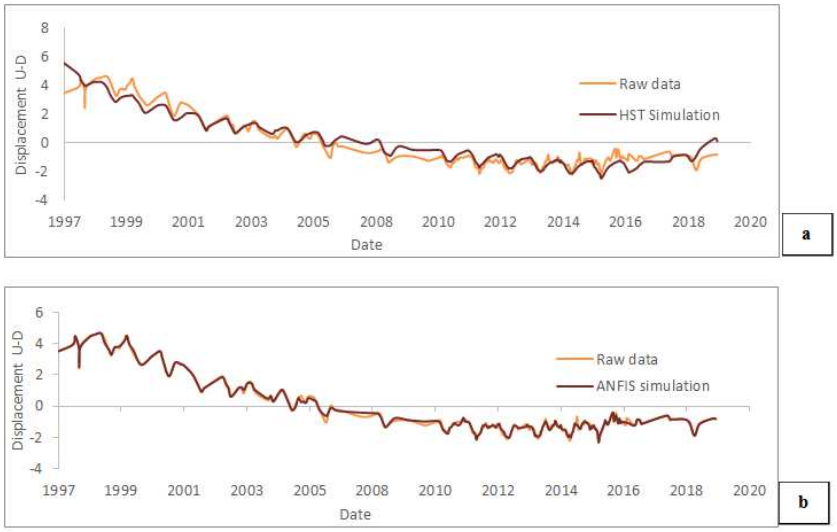

Figure 29. *Displacements from upstream to downstream measured (cm) on the pendulum P1D: (a) HST; (b) ANFIS.*

Overall, the behavior of the pendulum is well assimilated by the models, and as shown in the figures above, the errors are acceptable; nevertheless, the excellence of the model is mainly explained by the quality of the influences of the explanatory data which are the level of the reservoir, the season in the year and the time (HST). The statistical analysis of the influential parameters recorded in this pendulum is of good quality (correlation coefficient R^2 = 0.99412 for Upstream-Downstream and R^2 = 0.97767 for left-right). It shows the low influence of the season on the value of the measurements (4.949% contribution to the explanation of the phenomena for Upstream-Downstream and 17.236% for left-right – "Seasonal effects" graphs). The analysis shows an upward temporal drift, far too upward moreover, of the variations recorded on the pendulum (95.151% explanation for Upstream-Downstream and 92.095% for left-right) resulting in large movements unstabilized 7.44 cm for Upstream-Downstream and 7.11 cm for left-right in 20 years ("Time effects" graphs). A weakly explanatory hydrostatic effect (2.36% for Upstream-Downstream and 2.996% for left-right) resulting in a displacement of 0.39cm for a rise in the water level of 1m Upstream-Downstream and by a displacement of 0.1cm for a rise in the level of the water body of 1m in left-right bank (see "Hydrostatic Effect" graphs).

4.3.2. Displacements in the P3I Pendulum

Figures 30 and 31 highlight the evolution of displacements in the dam according to the years of service. The influence of the explanatory data of all the pendulums is illustrated through Table 6.

Figure 30. *Displacement (cm) Left-Right bank of the pendulum P3I: a) HST; b) ANFIS.*

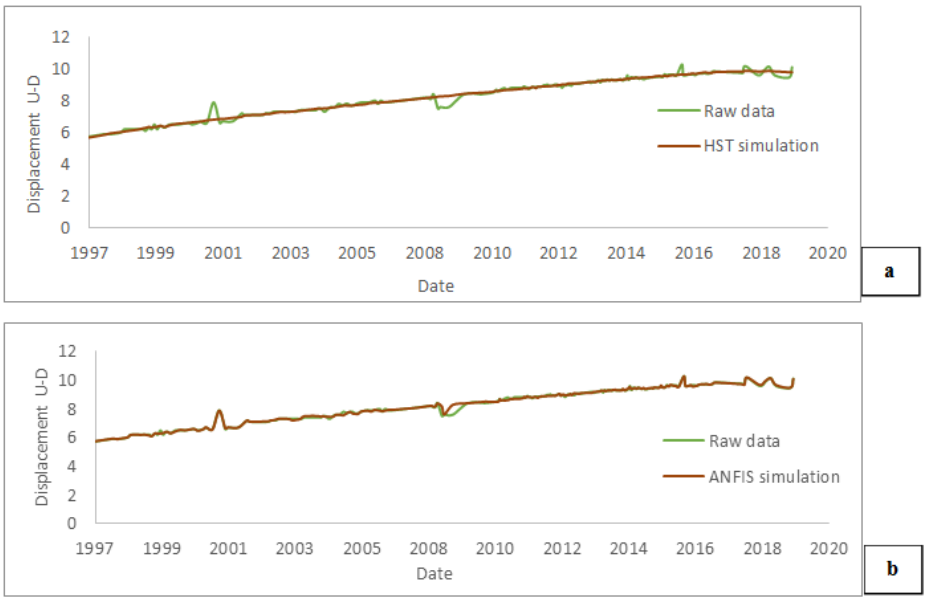

Figure 31. *Displacement (cm) of upstream-Downstream of pendulum P3I: a) HST; b) ANFIS.*

4.4. Relocation of the Spillway Dam

4.4.1. Pendulum E2-3D

Figures 32 and 33 show the evolution of the displacements recorded in this pendulum over the years.

Table 6 summarizes the influences of the reservoir coast, season and time in the E2-3D pendulum.

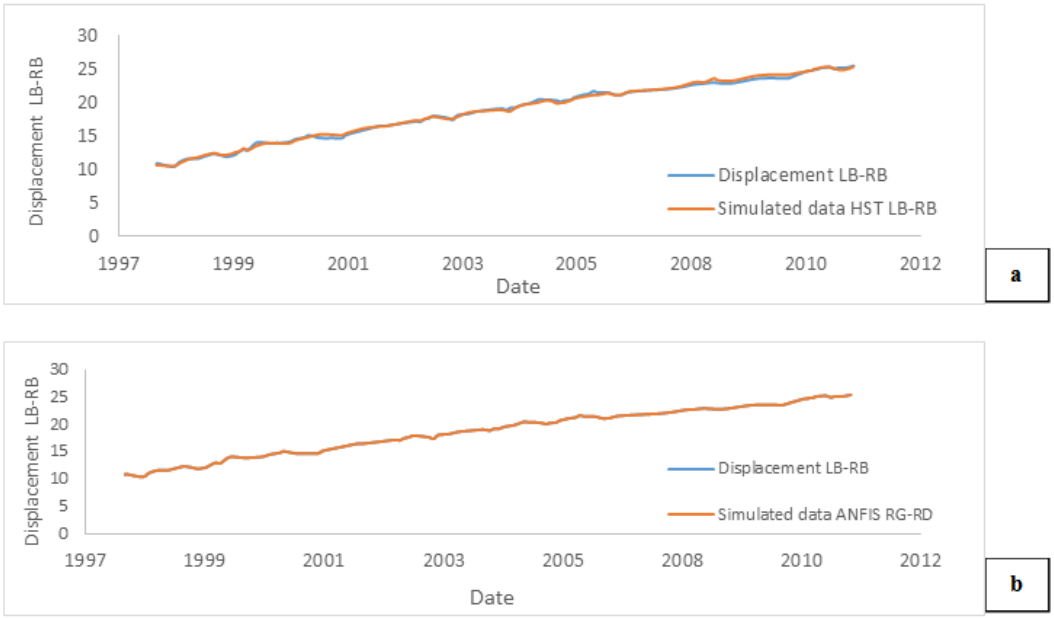

Figure 32. *Displacements (cm) of the Left-Right bank of the pendulum E2-3D.*

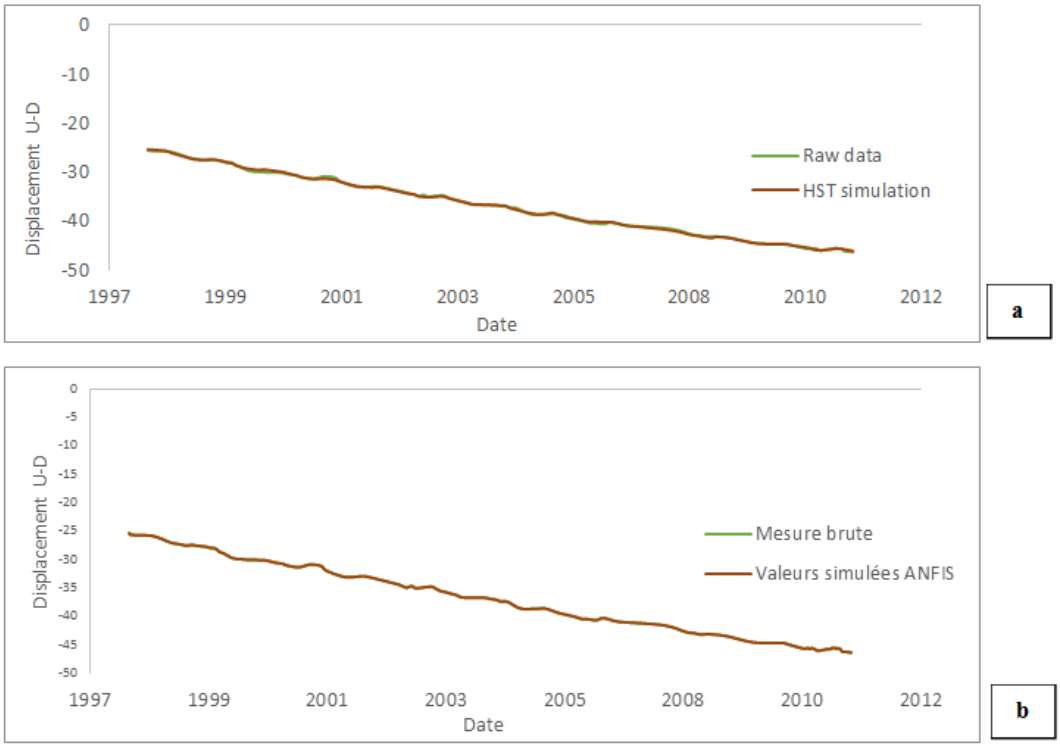

Figure 33. *Displacements (cm) upstream-downstream pendulum E2-3D: a) HST; (b) ANFIS.*

Table 6 summarizes the influences of the reservoir coast, season and time in the E2-3D pendulum.

4.4.2. Pendulum E6-7D

Tables 6 and 7 summarizes the influences of the reservoir coast, season and time in the E6-7D pendulum. Figures 34 and 35 show the evolution of displacements as a function of time.

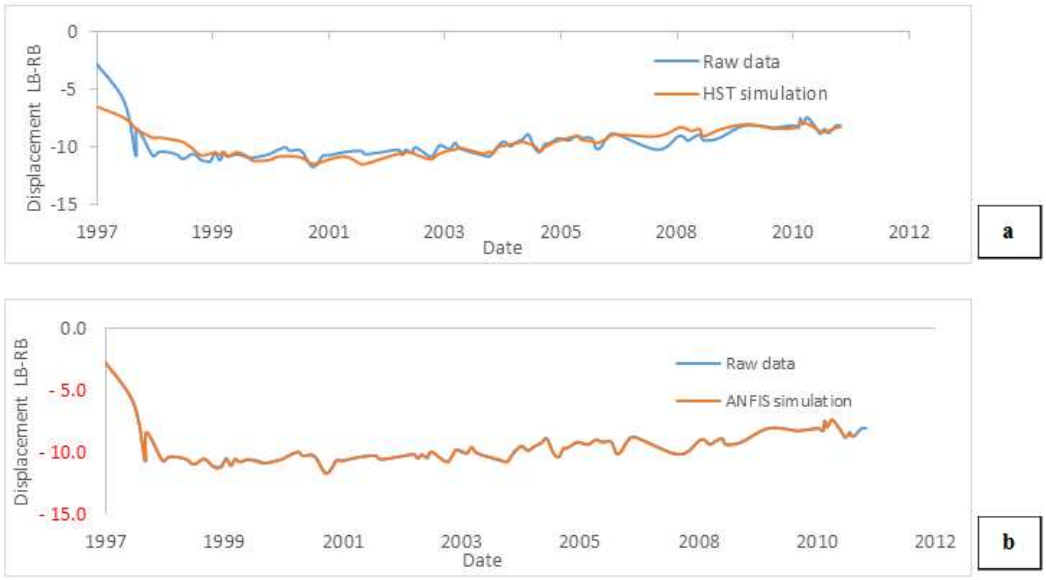

Figure 34. *Displacements (cm) Left-Right bank pendulum E6-7D: (a) HST; (b) ANFIS.*

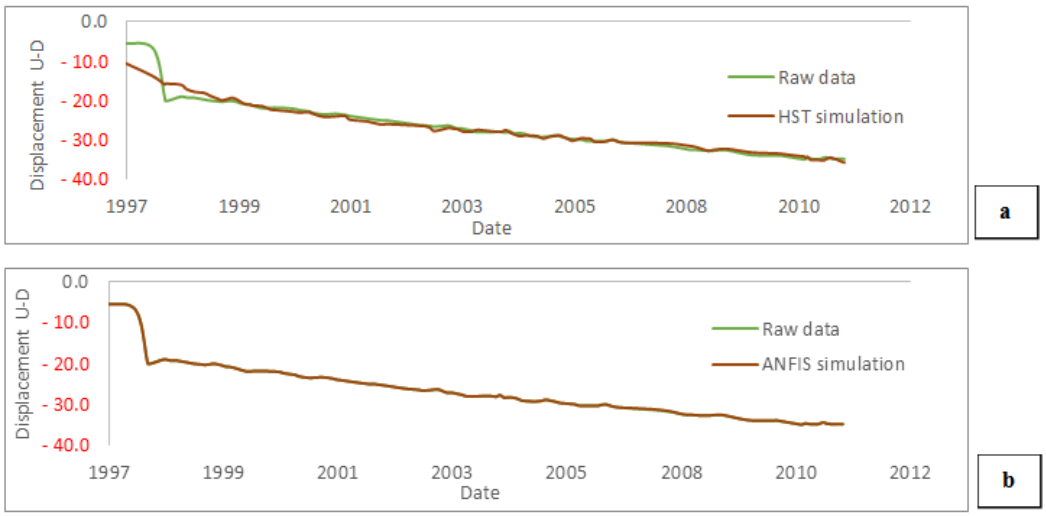

Figure 35. *Upstream-downstream displacements of pendulum E6-7D: (a) HST; (b) ANFIS.*

Table 6. *Evaluation of the performances of the different prediction models on all the pendulums.*

Pendulum	Model	HST	ANFIS
E6-7D	MSE	0.26480258	1.28E-05
	NASH	0.81610649	0.99999248
	R	0.84467056	0.99999248
	MAPE	-3.72081555	-0.02277325
E2-3D	MSE	0.0587672	1.47E-06
	NASH	0.99864049	0.99999997
	R	0.99864234	0.99999997
	MAPE	-0.51834962	-0.00160254
P5I	MSE	0.03667014	1.29E-08
	NASH	0.92078521	0.99999997
	R	0.9265996	0.99999997
	MAPE	2.16593849	0.00104804
P3I	MSE	0.02367039	0.00659559
	NASH	0.98203608	0.99505795
	R	0.98235309	0.99508281
	MAPE	2.46122631	1.20555695
P1D	MSE	0.41384878	0.01361954
	NASH	0.85262718	0.99575404
	R	0.87155629	0.99577299
	MAPE	-62.5843528	-3.36682009

Table 7. *Balance of influences for displacements (HST).*

PENDULUM	DISPLACEMENTS	R (%)	R-H (%)	R-S (%)	R-T (%)
E2_3	Upstream-downstream	99.700	2.761	4.586	92.352
	Left-Right bank	99.910	1.340	3.147	95.423
E6_7D	Upstream-downstream	89.250	12.664	21.098	55.488
	Left-Right bank	99.775	0.927	3.697	95.151
P1D	Upstream-downstream	99.412	2.367	4.949	92.095
	Left-Right bank	97.767	2.996	17.236	77.536
P3I	Upstream-downstream	42.699	2.096	3.111	37.493
	Left-Right bank	95.419	6.266	4.085	85.069
P5I	Upstream-downstream	69.262	13.155	9.166	46.942
	Left-Right bank	93.365	18.125	7.946	67.294
	Average Upstream-downstream	80.065	6.609	8.582	64.874
	Average Left-Right bank	97.247	5.931	7.222	84.095

The analysis of the monitoring data of the pendulums of the large earthen dam of Songloulou gives the results above. These results are presented in the form of graphs for each of the explanatory effects resulting from the associated statistical analysis. This analysis is of good quality (average correlation coefficient R^2 = 88.656%). It shows the low (average) influence of the season on the value of the measurements (7.902% contribution to the explanation of the phenomena). The analysis also shows an upward temporal drift, far too upward moreover, of the variations recorded on the pendulum (74.48% explanation) resulting in large unstabilized movements and a weakly explanatory hydrostatic effect (6.27%) for explanation. This very strong influence of time, although abnormal, is logically explained by the phenomena of alkali-reaction, which promotes accelerated aging of the structure. The presence of many cracks on the structure could also contribute. From the analysis of the data of the various pendulums, it appears that the displacements on the spillway dam are very important. This phenomenon is explained by the fact that this dam is affected by the alkali-aggregate reaction and by the fact of significant stresses during periods of flooding (openings and closings of the spillways).

5. Validation of the Model: Simulation of the Piezometric Heights on PLAXIS

PLAXIS is a Finite Element calculation code designed to perform any type of hydromechanical analysis for different types of geotechnical applications [37]. The water intake dam is modeled in 2-D plane strains representing its cross section, with triangular elements at 15 knots with high precision. All displacements and seepage or flow conditions are fixed at the bottom of the model. The mechanical behavior of the dam materials obeys of the Mohr-Coulomb failure criterion [38, 39]. Table 8 presents the mechanical parameters of the different materials of the water intake dam.

Table 8. *Parameters of foundation soil and earth dam materials.*

Material	γ_h	γ_{sat}	c'	Φ'	Young's modulus	Poisson's ratio	Coefficient of permeability
Unity	(kN/m^3)	(kN/ m^3)	(kPa)	(°)	(MPa)	(-)	(m/s)
Core	18	19	15	32	74	0.3	1.15741E-14
Rip-Rap	22	24	0	40	80	0.3	1.15741E-12
Filtered	19	22	0	40	400	0.3	2.3148E-12
Rockfill	22	24	0	45	800	0.3	1.15741E-12
Rock foundation	26	26	1000	45	5000	0.3	5.78704E-14

By averaging the different heights (real heights, HST and ANFIS heights) obtained during the different seasons, we use these heights as the hydraulic head on the main dam and we discuss which of the models best approximates the real results. The results of the modeling in cartographic form of displacements and stresses as a function of the water level in the dam are presented in the various models (Figures 36 to 44). Figure 36 presents the simulated horizontal displacements with the real levels of restraints, it is noted that figure 37 which presents the simulated horizontal displacements with the ANFIS heights is almost similar to figure 36, with a real maximum displacement of 380 mm and a maximum ANFIS displacement of 374 mm, on the other hand the displacements simulated with the HST heights are quite far from reality as shown in figure 38, which generate a maximum displacement of 213 mm (Table 9).

Table 9. *Results of numerical simulation and comparison the horizontal displacement obtained on the pendulums.*

Displacements and tresses	Piezometric level: 530 m	ANFIS heights	HST heights	Average measurements of pendulum
Maximal horizontal displacement (mm)	380	374	213	-
Horizontal displacement at the pendulums position (mm)	80	80	62	70
Maximal vertical displacement (mm)	159	159	130	-
Total stress (MPa)	34	34	34	-

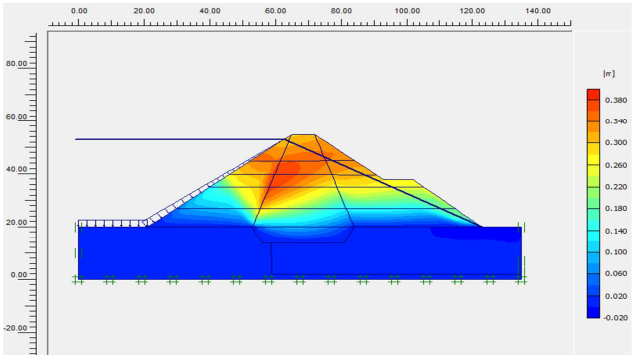

Figure 36. *Map of horizontal displacements obtained with simulated real heights.*

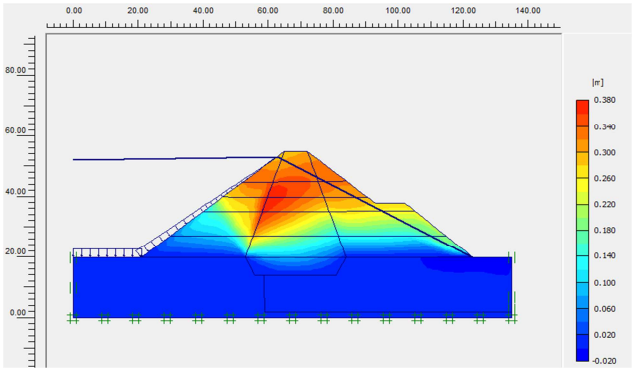

Figure 37*. Map of horizontal displacements obtained with simulated ANFIS heights.*

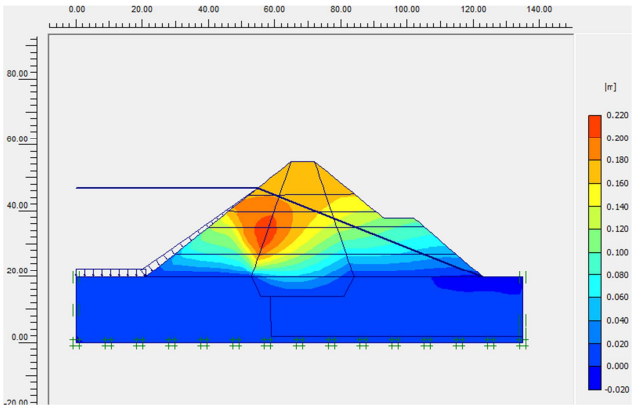

Figure 38. *Map of horizontal displacements obtained with simulated HST heights.*

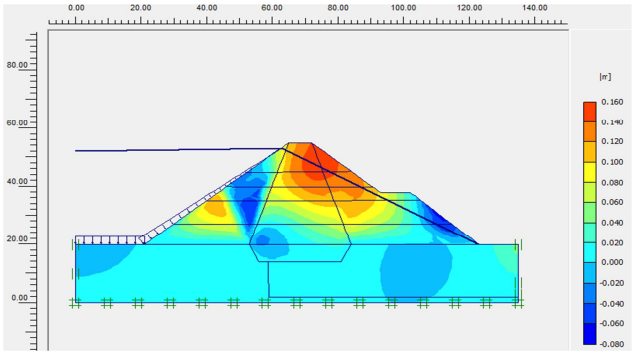

Figure 39. *Map of vertical displacements obtained with simulated real heights.*

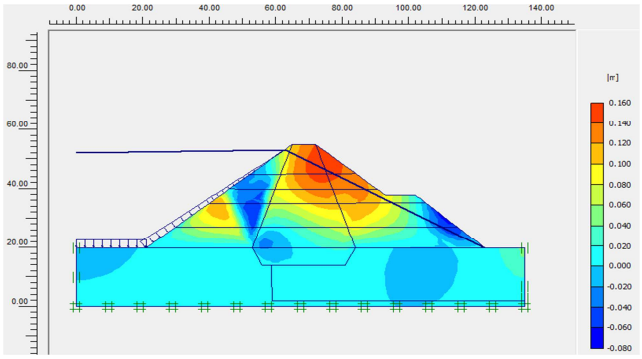

Figure 40. *Map of Vertical displacements obtained with simulated ANFIS heights.*

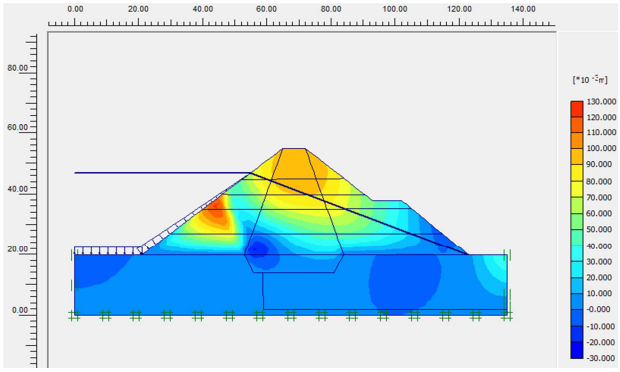

Figure 41. *Map of vertical displacements obtained with simulated HST heights.*

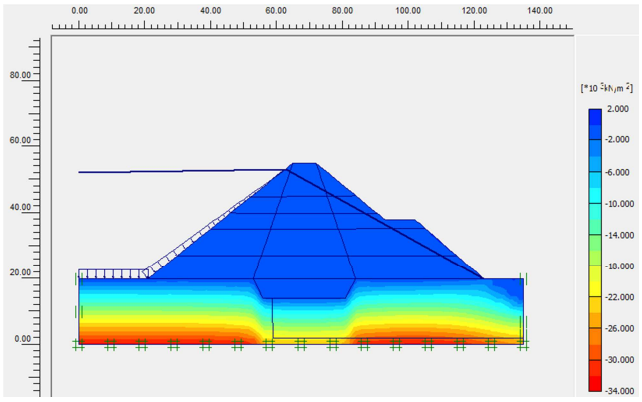

Figure 42. *Map of total stress obtained with simulated real heights.*

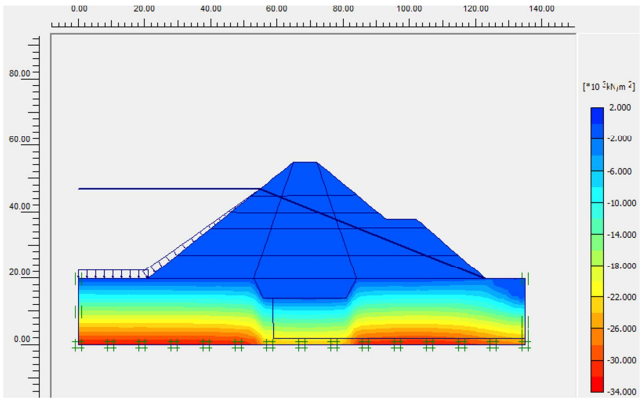

Figure 43. *Map of total stress obtained with simulated ANFIS heights.*

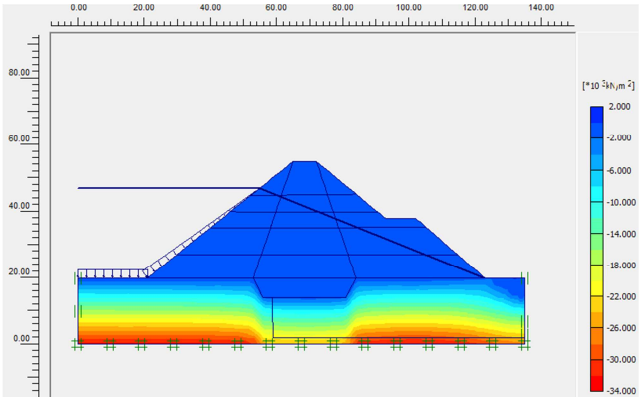

Figure 44. *Map of total stress obtained with simulated HST heights.*

Figure 39 presents the simulated vertical displacements with the actual reservoir levels, and Figure 40, with the data from the ANFIS model with a maximum actual displacement of 159 mm for both. Figure 41, on the other hand, represents the maximum vertical displacements (130 mm) for HST. On the other hand, the simulated displacements with the HST heights are quite far from reality as shown in figure 40, which generate a maximum displacement of 122 mm. The results of these modelings show a hydromechanical behavior in agreement with the monitoring data. The various tools used in this paper for the prediction of long-term behavior are very reliable, they allow through indicators of safety and reliability of the operation of the structure to anticipate possible risks which could compromise the good integrity of the geotechnical structures. This proposed method makes it possible to carry out all the calculations allowing the user to easily analyze and interpret the data recorded on the monitoring tools. These results presented not only facilitate the analysis but also offer the user the possibility of choosing between two analysis methods, namely ANFIS and HST. Obviously, we have set some comparison and validation criteria to be able to guide the discussions and guide the managers of the said structures in order to ensure their permanent operation in complete safety, security and reliability, whatever the severity of the environmental conditions.

6. Conclusion

It was a question in this work, to discuss as for the method of adequate analysis between the classical model HST and the fuzzy neuron model ANFIS while proposing an method capable of automatically processing these data in this direction, from our study it emerges: The prediction quality of each of the models unequivocally indicates a preference for the ANFIS model. However, when drawing conclusions from such a study, some caution should be exercised. Indeed, all comparisons between the two models are based on the inseparable data sets from the Songloulou large earthen dam. To validate our model, i.e. to know if it is capable of detecting an anomaly on the dam, it would be necessary to calibrate it using a set of data from a dam on which occurred in the past a failure. The analysis of the under pressure on the intake dam shows that the sealing layer separating the upstream part and the downstream part works and protects the downstream from the upstream well, however at the level of the spillway dam there is a significant increase in the piezometric level over time, which shows an increase in the amount of water infiltrated over the years.

The safety, security and reliability of dams depend on the lives of thousands of people, so we must be careful not to act hastily in this area. Consequently, it seems to us preferable to model each dam individually and to find in each case an adequate model, for certain structures, the classic model will certainly be more adequate, while for others, the ANFIS model will lead to better results both for the treatment of pressures and displacements. The introduction of the ANFIS model expands the range of models available to perform the necessary control and prediction work on dams. This model also offers an alternative to the classic model when the latter reveals some weaknesses and allows two different models to be used in a complementary way. To predict the overall behavior of the structure, it is necessary to use numerical modeling in order to assess all the inseparable parameters (displacements, pressures, seepages, leak rates, etc.). The modeling results are in perfect agreement with the displacements measured through pendulums.

References

[1] Bonelli S., Felix F., Jourmeni R., Carlier D. (1997). Auscultation des barrages en terre-Modélisation de l'effet pluie, colloque scientifique EC'97, Strasbourg, 22-23 mai.

[2] Royet Paul. (2006). La surveillance et l'entretien des petits barrages. Éditions du Cemagref.

[3] Lautrin D. (2003). Vieillissement et réhabilitation des petits barrages en terre. Éditions du Cemagref, 240 p.

[4] Anton S., Pougatsch H. (2011). Les barrages-du projet à la mise en service. *Presses Polytechniques et Universitaires Romandes (PPUR),* Ecole Polytechnique Fédérale de Lausanne, 714p.

[5] Bourdarot E., Carrère A. J., Hoonakker M. (2000). Apports combinés de l'auscultation et de la modélisation pour l'analyse et la compréhension des barrages, XXe Congrès CIGB. - Beijing, 2000.

[6] Bonelli S., Royet P. (2001). Delayed response analysis of dam monitoring data, ICOLD European Symposium, Geiranger, Norway, 25-27 June 2001.

[7] Bonelli S. (2007). Delayed response analysis of dam monitoring data. Edité par Cemagref, juillet 2007.

[8] Bonelli S., Félix H., Tourment R. (1998). Fiabilité des matériaux et des structures, Interprétation des mesures d'auscultation des barrages par régression linéaire multiple «HST», 2e conférence nationale JN-FIAB'98.

[9] Plancke V. (1997). Auscultation des barrages, logiciel de traitement statistique des mesures, mémoire ENIIRS, Cemagref.

[10] Zoa A., Amba J. C., Mbelen F. X. (2020). Monitoring and numerical modeling of the full scale experimental embankment on soft Douala clays of Cameroon. *International Journal of Civil Engineering and Technology,* volume 11, no. 7.

[11] Dardanelli G., La Loggia G., Perfeti N., Fulvio C., Luigi P. A. (2014). Monitoring displacements of an earthen dam using GNSS and remote sensing. *Remote sensing for Agriculture, Ecosystems, and Hydrology XVI 9239*, pp. 574-589.

[12] Gikas V., Sakellariou M. (2008). Settlement analysis of the Mornos earth dam (Greece): Evidence from numerical modeling and geodetic monitoring. *Engineering Structures 30 (11),* pp. 3074-3081.

[13] Gikas V., Sakellariou M. (2008). Horizontal deflection analysis of a large earthen dam by means of geodetic and geotechnical methods. *13th FIG International symposium on deformation measurements and analysis and 4th IAG symposium on geodesy for geotechnical and structural engineering*.

[14] Szostack-Chrzanowski A., Massiéra M. (2006). Relation between monitoring and design aspect of large earth dams; *Proceedings, 3rd IAG Symposium of Geodesy for Geotechnical and Structural Engineering and 12th FIG symposium on Deformation measurements*. Baden Australia.

[15] Mouyeaux A., Carvajal C., Bressolette P., Peyras L., Breul P., Bacconnet C. (2018). Probabilistic stability analysis of an earth dam by Stochastic Finite Element Method based on field data. *Computers and Geotechnics*, *101*, 34-47.

[16] Guo X., Dias, D. Carvajal C., Peyras L., Breul P. (2018). Reliability analysis of embankment dam sliding stability using the sparse polynomial chaos expansion. *Engineering Structures*, *174*, 295-307.

[17] Bal L., Buyle-Bodin F. (2013). Artificial neural network for predicting drying shrinkage of concrete. *Construction and Building Materials*, *38*, 248-254.

[18] Pang, R., Xu, B., Kong, X., Zou, D., & Zhou, Y. (2018). Seismic reliability assessment of earth-rockfill dam slopes considering strain-softening of rockfill based on generalized probability density evolution method. *Soil Dynamics and Earthquake Engineering*, *107*, 96-107.

[19] Campos, A., Lopez, C. M., Blanco, A., & Aguado, A. (2018). Effects of an internal sulfate attack and an alkali-aggregate reaction in a concrete dam. *Construction and Building Materials*, *166*, 668-683.

[20] Doghai Liu, Bo Cui, Yugang Liu, Denghua zhong (2013). Automatic control and real-time monitoring system for earth-rock dam material truck watering. *Automation in Construction 30*, pp. 70-80.

[21] Cejka F., Benes V., Glac F., Boukalova Z. (2018). Monitoring of seepages in earthen dams and levees. *International Journal of Environmental Impacts* 1 (3), pp. 267-278.

[22] Krzysztof Radzicki, Stephane Bonelli (2010). Thermal seepage monitoring in the earth dams with impulse response function analysis model. *Na*.

[23] Inaudi D., Church J. (2011). Paradigm shifts in monitoring levees and earth dams distributed fiber optic monitoring systems. *31st USSD Annual Meeting & Conference*, San Diego, California, USA.

[24] Pagano L., Sica S. (2013). Earthquake early warning for earth dams: Concepts and objectives. *Natural hazards*, 66 (2), 303-318.

[25] Di Martire D., Iglesias Ruben., Monells D., Centolanza G., Sica S. (2014). Comparison between differential SAR interferometry and ground measurements data in the displacement monitoring of the earth-dam of Conza della Campania (Italy). *Remote sensing of environment, 148*, pp. 58-69.

[26] Andreini, M., Gardoni, P., Pagliara, S., & Sassu, M. (2019). Probabilistic models for the erosion rate in embankments and reliability analysis of earth dams. *Reliability Engineering & System Safety*, *181*, 142-155.

[27] Guillemot T., Lino M., Nzali E. (2013). Diagnostic et mise en sécurité du barrage de Songlou au Cameroun vis-à-vis des désordres liés à l'alcali-réaction. Colloque technique, Modernisation des barrages, CFBR, 10p.

[28] Ferry S., William G. (1958). Méthodes d'analyse et de surveillance des déplacements observés par le moyen de pendules dans les barrages. VIth International Congress on Large Dams, New-York, vol. II, ICOLD, 1958, pp. 1179-1201.

[29] Touzet C. (1992). Les réseaux de neurones artificiels, introduction au connexionnisme: cours et exercices et travaux pratiques: Collection de l'EERIE.

[30] Abrahart R. J., See L. M., Kneale P. E. (2005). Neural network for hydrological modelling: Taylor & Francis e-Library.

[31] Godjevac J. (1999). Idées nettes sur la logique floue. *Presses Polytechniques et Universitaires Romandes*.

[32] Chuen C. (1990). Fuzzy Logic in Control Systems: Fuzzy Logic Controller, part I. IEEE Transactions on System Mann. And cyri Rsetrs, Vol. 20 No. 2, March/April 1990, pp: 405-417.

[33] Chuen C. (1990). Fuzzy Logic in Control Systems: Fuzzy Logic Controller, part II" IEEE Transactions on System Mann. And cyri Rsetr, Vol. 20 No. 2, March/April 1990 pp: 419-435.

[34] Rafael A., Gouriveau M., Zerhouni N., (2008). Pronostic de défaillances: maitrise de l'erreur de prédiction, Manuscrit auteur, publié dans 7ème Conférence Internationale de Mobilisation et Simulation, MOSIM'08, Paris, France.

[35] MATLAB (2019). MATLAB Software Development Tools.

[36] Zoa A., Amba J. C. (2020). Assessment of stiffness and strength parameters for the soft soil Model of clays of Cameroon. *Hindawi, International Journal Advances in Civil Engineering,* volume 2020.

[37] PLAXIS© (2018). Finite Element Code for Soil and Rock Analysis. Material Models Manual. v. 8, 256 p.

[38] Davis R. O., Selvadurai A. P. S. (2002). *Plasticity and Geomechanics*, Cambridge University Press.

[39] Hill R. (1998). *The Mathematical Theory of Plasticity*, Oxford University Press, U.S.A.